TAE buffer for electrophoresis. The gel was stained with ethidium bromide and DNA was visualized under UV light.

H_2O_2 treatment

M. smegmatis strains were grown to an OD600 of 0.5 to 0.7 in LB medium at 37°C. The bacterial culture was then diluted to 0.1 OD by the medium for the assay. The reaction was initiated by adding a final concentration of 12.5 mM H_2O_2 and incubated for 0, 1, or 2 hours. If necessary, bacteria were pretreated with 40 mM desferal (Sigma) for 5 min before exposure to H_2O_2. At each time point, the bacterial suspension was serially diluted using sterilized water and plated onto LB agar (Sigma). Living bacteria were enumerated by counting CFU after incubation at 37°C for 4–6 days.

Supporting Information

Figure S1 MDP1/ML-LBP homologues. Blast search was performed for amino acid sequence of BCG-MDP1 against all protein database using the National Center for Biotechnology Information's (NCBI) BLAST server and proteins with over 150 of total score are aligned. Conserved domain of Integration host factor (IHF) and HU were shown by yellow box, which was identified with domain search using NCBI server. MDP1-specific DNA binding region [20] that interacts with GC-rich DNA was indicated by red.
(DOC)

Figure S2 Ferroxidase activity of Ms-MDP1. The conversion from Fe^{2+} to Fe^{3+} was scanned by measuring the absorbance at 305 nm. Black line, 0.4 mM $FeSO_4$; blue line, 0.4 mM $FeSO_4$+1.4 μM Histone H1; red line, 0.4 mM $FeSO_4$+1.4 μM Ms-MDP1.
(TIF)

Figure S3 Ferroxidase activity of Mtb-MDP1 and ferritin using hydroxyl peroxide, as the oxidant The conversion from Fe^{2+} to Fe^{3+} was monitored by spectral analysis at 305 nm. Hydroxyl peroxide (6–108 mM) were added to the solution of either 0.5 μM Mtb-MDP1 (A) or horse ferritin (B) including with 21 μM $FeSO_4$.
(TIF)

Acknowledgments

We are grateful to Dr. Thomas Dick, Novartis Institute for Tropical Diseases, for providing Ms-MDP1/HLP-KO *M. smegmatis*. We also thank Sara Matsumoto for assistance with the experiments and heartfelt encouragement.

Author Contributions

Conceived and designed the experiments: MT MO-O MI KI TA HO K. Kobayashi AR SM. Performed the experiments: MT MO-O EFS K. Kitadokoro YN MYN YS SM. Analyzed the data: MT MO-O MI KI TA HO K. Kobayashi AR SM. Wrote the paper: MT MO-O EFS K. Kobayashi AR SM.

References

1. Chiancone E, Ceci P, Ilari A, Ribacchi F, Stefanini S (2004) Iron and proteins for iron storage and detoxification. Biometals 17: 197–202.
2. Banyard SH, Stammers DK, Harrison PM (1978) Electron density map of apoferritin at 2.8-A resolution. Nature 271: 282–284.
3. Carrondo MA (2003) Ferritins, iron uptake and storage from the bacterioferritin viewpoint. EMBO J 22: 1959–1968.
4. Bozzi M, Mignogna G, Stefanini S, Barra D, Longhi C, et al. (1997) A novel non-heme iron-binding ferritin related to the DNA-binding proteins of the Dps family in Listeria innocua. J Biol Chem 272: 3259–3265.
5. Ilari A, Stefanini S, Chiancone E, Tsernoglou D (2000) The dodecameric ferritin from Listeria innocua contains a novel intersubunit iron-binding site. Nat Struct Biol 7: 38–43.
6. Bou-Abdallah F, Lewin AC, Le Brun NE, Moore GR, Chasteen ND (2002) Iron detoxification properties of Escherichia coli bacterioferritin. Attenuation of oxyradical chemistry. J Biol Chem 277: 37064–37069.
7. Cirillo SL, Subbian S, Chen B, Weisbrod TR, Jacobs WR, Jr., et al. (2009) Protection of *Mycobacterium tuberculosis* from reactive oxygen species conferred by the mel2 locus impacts persistence and dissemination. Infect Immun 77: 2557–2567.
8. Boelaert JR, Vandecasteele SJ, Appelberg R, Gordeuk VR (2007) The effect of the host's iron status on tuberculosis. J Infect Dis 195: 1745–1753.
9. De Voss JJ, Rutter K, Schroeder BG, Su H, Zhu Y, et al. (2000) The salicylate-derived mycobactin siderophores of *Mycobacterium tuberculosis* are essential for growth in macrophages. Proc Natl Acad Sci USA 97: 1252–1257.
10. Barry CE, 3rd, Boshoff H (2005) Getting the iron out. Nat Chem Biol 1: 127–128.
11. Gold B, Rodriguez GM, Marras SA, Pentecost M, Smith I (2001) The *Mycobacterium tuberculosis* IdeR is a dual functional regulator that controls transcription of genes involved in iron acquisition, iron storage and survival in macrophages. Mol Microbiol 42: 851–865.
12. Gupta V, Gupta RK, Khare G, Salunke DM, Tyagi AK (2009) Crystal structure of Bfr A from *Mycobacterium tuberculosis*: incorporation of selenomethionine results in cleavage and demetallation of haem. PLoS One 4: e8028.
13. Pessolani MC, Smith DR, Rivoire B, McCormick J, Hefta SA, et al. (1994) Purification, characterization, gene sequence, and significance of a bacterioferritin from *Mycobacterium leprae*. J Exp Med 180: 319–327.
14. Cole ST, Eiglmeier K, Parkhill J, James KD, Thomson NR, et al. (2001) Massive gene decay in the leprosy bacillus. Nature 409: 1007–1011.
15. Cole ST, Brosch R, Parkhill J, Garnier T, Churcher C, et al. (1998) Deciphering the biology of *Mycobacterium tuberculosis* from the complete genome sequence. Nature 393: 537–544.
16. Colangeli R, Haq A, Arcus VL, Summers E, Magliozzo RS, et al. (2009) The multifunctional histone-like protein Lsr2 protects mycobacteria against reactive oxygen intermediates. Proc Natl Acad Sci USA 106: 4414–4418.
17. Matsumoto S, Yukitake H, Furugen M, Matsuo T, Mineta T, et al. (1999) Identification of a novel DNA-binding protein from *Mycobacterium bovis* bacillus Calmette-Guerin. Microbiol Immunol 43: 1027–1036.
18. Shimoji Y, Ng V, Matsumura K, Fischetti VA, Rambukkana A (1999) A 21-kDa surface protein of *Mycobacterium leprae* binds peripheral nerve laminin-2 and mediates Schwann cell invasion. Proc Natl Acad Sci USA 96: 9857–9862.
19. Aoki K, Matsumoto S, Hirayama Y, Wada T, Ozeki Y, et al. (2004) Extracellular mycobacterial DNA-binding protein 1 participates in *Mycobacterium*-lung epithelial cell interaction through hyaluronic acid. J Biol Chem 279: 39798–39806.
20. Furugen M, Matsumoto S, Matsuo T, Matsumoto M, Yamada T (2001) Identification of the mycobacterial DNA-binding protein 1 region which suppresses transcription in vitro. Microb Pathog 30: 129–138.
21. Matsumoto S, Matsumoto M, Umemori K, Ozeki Y, Furugen M, et al. (2005) DNA augments antigenicity of mycobacterial DNA-binding protein 1 and confers protection against *Mycobacterium tuberculosis* infection in mice. J Immunol 175: 441–449.
22. Katsube T, Matsumoto S, Takatsuka M, Okuyama M, Ozeki Y, et al. (2007) Control of cell wall assembly by a histone-like protein in Mycobacteria. J Bacteriol 189: 8241–8249.
23. Matsumoto S, Furugen M, Yukitake H, Yamada T (2000) The gene encoding mycobacterial DNA-binding protein I (MDPI) transformed rapidly growing bacteria to slowly growing bacteria. FEMS Microbiol Lett 182: 297–301.
24. Davis TM, Wilson WD (2000) Determination of the refractive index increments of small molecules for correction of surface plasmon resonance data. Anal Biochem 284: 348–353.
25. Hesse L, Beher D, Masters CL, Multhaup G (1994) The beta A4 amyloid precursor protein binding to copper. FEBS Lett 349: 109–116.
26. Imada I, Sato EF, Miyamoto M, Ichimori Y, Minamiyama Y, et al. (1999) Analysis of reactive oxygen species generated by neutrophils using a chemiluminescence probe L-012. Anal Biochem 271: 53–58.
27. Sassetti CM, Boyd DH, Rubin EJ (2003) Genes required for mycobacterial growth defined by high density mutagenesis. Mol Microbiol 48: 77–84.
28. Lewin A, Baus D, Kamal E, Bon F, Kunisch R, et al. (2008) The mycobacterial DNA-binding protein 1 (MDP1) from *Mycobacterium bovis* BCG influences various growth characteristics. BMC Microbiol 8: 91.
29. Lee BH, Murugasu-Oei B, Dick T (1998) Upregulation of a histone-like protein in dormant *Mycobacterium smegmatis*. Mol Gen Genet 260: 475–479.
30. Brooks BW, Young NM, Watson DC, Robertson RH, Sugden EA, et al. (1991) *Mycobacterium paratuberculosis* antigen D: characterization and evidence that it is a bacterioferritin. J Clin Microbiol 29: 1652–1658.
31. Inglis NF, Stevenson K, Hosie AH, Sharp JM (1994) Complete sequence of the gene encoding the bacterioferritin subunit of Mycobacterium avium subspecies silvaticum. Gene 150: 205–206.

32. Janowski R, Auerbach-Nevo T, Weiss MS (2008) Bacterioferritin from Mycobacterium smegmatis contains zinc in its di-nuclear site. Protein Sci 17: 1138–1150.
33. Soares de Lima C, Zulianello L, Marques MA, Kim H, Portugal MI, et al. (2005) Mapping the laminin-binding and adhesive domain of the cell surface-associated Hlp/LBP protein from *Mycobacterium leprae*. Microbes Infect 7: 1097–1109.
34. Gobin J, Horwitz MA (1996) Exochelins of *Mycobacterium tuberculosis* remove iron from human iron-binding proteins and donate iron to mycobactins in the *M. tuberculosis* cell wall. J Exp Med 183: 1527–1532.
35. Gobin J, Moore CH, Reeve JR, Jr., Wong DK, Gibson BW, et al. (1995) Iron acquisition by *Mycobacterium tuberculosis*: isolation and characterization of a family of iron-binding exochelins. Proc Natl Acad Sci USA 92: 5189–5193.
36. Andrews SC, Robinson AK, Rodriguez-Quinones F (2003) Bacterial iron homeostasis. FEMS Microbiol Rev 27: 215–237.
37. Farhana A, Kumar S, Rathore SS, Ghosh PC, Ehtesham NZ, et al. (2009) Mechanistic insights into a novel exporter-importer system of *Mycobacterium tuberculosis* unravel its role in trafficking of iron. PLoS One 3: e2087.
38. Bradford MM (1976) A rapid and sensitive method for the quantitation of microgram quantities of protein utilizing the principle of protein-dye binding. Anal Biochem 72: 248–254.
39. Eisenthal R, Cornish-Bowden A (1974) The direct linear plot. A new graphical procedure for estimating enzyme kinetic parameters. Biochem J 139: 715–720.

Vaccine 29 (2011) 6881–6887

Contents lists available at ScienceDirect

Vaccine

journal homepage: www.elsevier.com/locate/vaccine

Loss of anti-mycobacterial efficacy in mice over time following vaccination with *Mycobacterium bovis* bacillus Calmette-Guérin

Yuriko Ozeki[a,b,*], Yukio Hirayama[a], Takemasa Takii[c], Saburo Yamamoto[d], Kazuo Kobayashi[e], Sohkichi Matsumoto[a,**]

[a] Department of Bacteriology, Osaka City University Graduate School of Medicine, 1-4-3 Asahimachi, Abeno-ku, Osaka 545-8585, Japan
[b] Department of Food and Nutrition, Sonoda Women's University, 7-29-1 Minamitsukaguchi-cho, Amagasaki, Hyogo, Japan
[c] Department of Molecular Health Sciences, Graduate School of Pharmaceutical Sciences, Nagoya City University, 3-1 Tanabe, Mizuho, Nagoya 467-8603, Japan
[d] Japan BCG Central Laboratory, 3-1-5 Matsuyama, Kiyose, Tokyo 204-0022, Japan
[e] Department of Immunology, National Institute of Infectious Diseases, 1-23-1 Toyama, Shinjuku-ku, Tokyo 162-8640, Japan

ARTICLE INFO

Article history:
Received 30 April 2011
Received in revised form 10 July 2011
Accepted 16 July 2011
Available online 29 July 2011

Keywords:
Mycobacterium
Vaccine
Adult pulmonary tuberculosis
BCG
Cellular immunity
TH1

ABSTRACT

Mycobacterium bovis bacillus Calmette-Guérin (BCG) is the most often used vaccine worldwide and sole vaccine against tuberculosis. BCG is protective against severe form of childhood tuberculosis but less or not protective to adult pulmonary tuberculosis. Therefore, improved vaccination strategies and development of new tuberculosis vaccines are urgent demands. For those purposes, appropriate animal models that reflect human are critically useful. However, in animal models, BCG vaccination protects well against subsequent challenge of *Mycobacterium tuberculosis*. In this study we evaluated the duration of protective efficacy of the BCG vaccination in mice over time and found that efficacy was diminished 40 weeks after vaccination. The aged mice older than 45 weeks are protected sufficiently after the vaccination with BCG, suggesting that loss of its efficacy is not dependent on the age of mice but rather depends on the period from vaccination. The loss of protection occurred in TH1 polarized STAT6 deficient mice despite the maintenance of interferon (IFN)-gamma production activity of lymph node cells and splenic $CD4^+$ T cells against *M. tuberculosis* antigens. Our data suggest that the duration from vaccination may explain the variation in BCG efficacy against adult pulmonary tuberculosis.

1. Introduction

Tuberculosis remains a serious threat for human health worldwide, where around 9.4 million people develop tuberculosis and 1.8 million people die each year [1].

Mycobacterium bovis bacillus Calmette-Guérin (BCG) is an attenuated strain of *M. bovis* [2] and the only currently available vaccine against tuberculosis. Nowadays it is accepted that BCG is effective for severe forms of childhood tuberculosis, such as disseminated tuberculosis and meningitis, but the efficacy for pulmonary tuberculosis in adults is variable among different populations and studies [3], and ineffectiveness was reported by controlled trials of over one hundred thousand people in India [2]. Poor or lack of efficacy of BCG for adult pulmonary tuberculosis is a serious problem in controlling the disease [2,4], because many deaths from tuberculosis are caused in adults and pulmonary tuberculosis is the most frequent clinical entity of tuberculosis. Several factors, such as strain variation [5], immune disturbance by exposure to environmental mycobacteria [6], and methodological discrepancies [7], are thought to be involved in the variation of effectiveness of BCG for adult pulmonary tuberculosis. In addition, decline of BCG efficacy with time was reported in human studies [8,9], implying that the duration of time from vaccination is related with the poor effectiveness of BCG in adult tuberculosis, although one study reported that it maintains over 50 years after vaccination [10].

In animal models, including mice, BCG vaccination induces a remarkable protection against subsequent challenge with *M. tuberculosis*. IFN-gamma is considered as a key cytokine [11–13] and IFN-gamma-producing $CD4^+$ T-helper 1 cells (TH1) play a pivotal role in the acquired protective immunity induced by BCG vaccination. In addition, the importance of IFN-gamma signaling pathways, such as the mutation of interferon-gamma receptors, in defense against mycobacterial infection is demonstrated by human studies [14,15].

Abbreviations: APCs, antigen-presenting cells; BCG, *Mycobacterium bovis* bacillus Calmette-Guérin; CFUs, colony forming units; KM, kanamycin; TH1, type 1 $CD4^+$ T-helper cells; TH2, type 2 $CD4^+$ T-helper cells.

* Corresponding author at: Department of Bacteriology, Osaka City University Graduate School of Medicine, 1-4-3 Asahi-machi, Abeno-ku, Osaka 545-8585, Japan. Tel.: +81 6 6645 3746; fax: +81 6 6645 3747.
** Corresponding author. Tel.: +81 6 6645 3746; fax: +81 6 6645 3747.
E-mail addresses: yuriozeki@med.osaka-cu.ac.jp (Y. Ozeki), sohkichi@med.osaka-cu.ac.jp (S. Matsumoto).

0264-410X/$ – see front matter © 2011 Elsevier Ltd. All rights reserved.
doi:10.1016/j.vaccine.2011.07.051

The aim of this study was to clarify the efficacious duration of BCG vaccination and immune responses in mice vaccinated with BCG. Although it is believed that BCG always confers protection against subsequent challenge of mycobacteria in animal models, we found that BCG efficacy was diminished 40 weeks after vaccination. The decline of protection is dependent on the time after BCG vaccination but not the age of mice. The loss of protection occurred even while maintaining IFN-gamma-productivity by $CD4^+$ T cells upon stimulation with *M. tuberculosis* antigens. Our data suggest the duration of time from vaccination may influence the variability of BCG efficacy against adult pulmonary tuberculosis.

2. Materials and methods

2.1. Animals

Female C57BL/6 and BALB/c mice were purchased from SLC (Shizuoka, Japan). STAT6-deficient BALB/c mice were purchased from the Jackson Laboratory (Bar Harbor, ME) and bred and maintained. Female C57BL/6, STAT6-deficient, and BALB/c mice of 6–8-weeks-old were used in the experiments. For the analysis of age effects in vaccination, we used female C57BL/6 mice aged 45–55 weeks old. Experiments were conducted according to the standard guidelines for animal experiments of Osaka City University Graduate School of Medicine.

2.2. BCG vaccination and challenge with kanamaycin-resistant BCG

C57BL/6, BALB/c, and STAT6-deficient mice were vaccinated via the peritoneal route with 10^5 colony-forming units (CFUs) of BCG suspended in 100 μL of sterilized phosphate-buffered saline (PBS). At various times after vaccination, lungs, livers, and spleens were homogenized in 1 mL sterile distilled water and serial dilutions were plated on Middlebrook 7H11 agar containing oleic acid, dextrose, albumin, and catalase enrichment (Difco) (7H11-OADC agar). CFUs were counted after culturing at 37 °C for 20–30 days. In some experiments, mice were intratracheally challenged with $5 \times 10^{4-5}$ CFUs of kanamycin (KM) resistant BCG suspended in 50 μL of PBS at 3, 20, and 40 weeks postvaccination. Five weeks later, lungs were homogenized as described above and serial dilutions of homogenates were plated on 7H11-OADC agar containing 10 μg/mL of KM.

2.3. Culture of lymph node cells and $CD4^+$ T cells in vitro

Axillary lymph nodes were obtained from at least three mice per group and single cell suspensions were prepared in Hanks' balanced salt solution by gently teasing the nodes between the frosted ends of two glass slides. This procedure routinely provided single cell suspensions with 90–95% viability as assessed by trypan blue dye exclusion. Lymph node cells were cultured in RPMI 1640 medium containing 10% heat-inactivated fetal calf serum, 2 mM L-glutamine, 100 U/mL penicillin and 100 μg/mL streptomycin (Life Technologies, Grand Island, NY). In some experiments, $CD4^+$ T cells were isolated from mice using a $CD4^+$ T Cell Isolation Kit (Miltenyl Biotec, Bergisch Gladgach, Germany) after erythrocyte depletion using 0.83% ammonium chloride solution. Obtained cells were labeled with PE-conjugated anti-CD4 mAb (eBioscience) and analyzed by flow cytometry. The purity of selected populations was confirmed as >96%. Non-$CD4^+$ cells retained in elution were incubated for over 2 h. Attached cells were used as antigen-presenting cells (APCs) after irradiation (20 Gy).

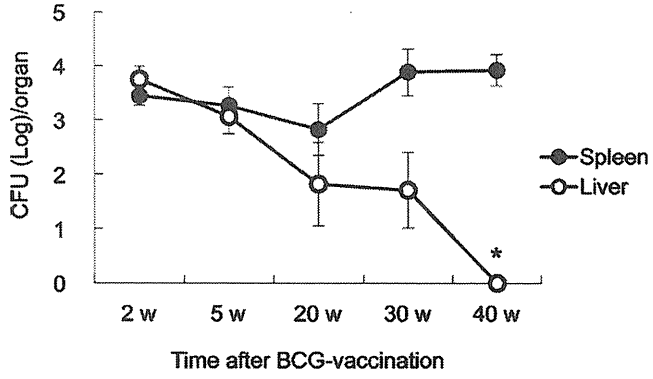

Fig. 1. Time course of surviving BCG number after vaccination. C57BL/6 mice were intraperitoneally vaccinated with 10^5 CFU of BCG. Various times after vaccination, bacterial numbers in livers (open circles) and spleens (closed circles) were monitored. Data represent mean values ± SD for 3–5 mice per group. *$P < 0.05$ versus CFU at 2 weeks after vaccination.

2.4. In vitro T-cell proliferation assay and measurement of cytokine secretion

Lymph nodes cells were resuspended at 2.5×10^6 cells/mL, $CD4^+$ T cells at 6×10^5 cells/mL and APCs at 2×10^5 cells/mL. Cells were cultured for 5 or 7 days with or without 10 μg/mL of purified protein derivatives (PPD, Japan BCG Laboratory, Tokyo) in 96-well plates in RPMI 1640 supplemented with 10% fetal calf serum (FCS), 2 mM L-glutamine, penicillin (100 U/mL), streptomycin (100 μg/mL) and 50 mM 2-mercaptoethanol. Proliferation was evaluated by pulsing the cells with 1 μCi (37 kBq)/well ^3H thymidine for 6 h and measuring ^3H thymidine incorporation using a scintillation counter. Production of IFN-gamma, interleukin (IL)-4, IL-5, and IL-10 in the culture supernatant was measured using commercially available ELISA kits (R&D System, Minneapolis, MN).

2.5. Statistical analysis

Results were analyzed by one-way analysis of variance (ANOVA) using SAS system R.8.1. Data were expressed as mean values ± standard deviation (SD) and considered significant if $P < 0.05$.

3. Results

3.1. Loss of protection induced by BCG vaccination in mice

Anti-tuberculosis immunity can be induced by vaccination with viable but not dead BCG [11,16]. First, in order to know if the survival rate of inoculated BCG correlated with protection, we examined how long BCG is sustained *in vivo*. We inoculated 10^5 CFU of BCG into C57BL/6 mice intraperitoneally and counted bacterial CFUs in organs, such as spleens, livers, and lungs. Although BCG was almost undetectable in lungs during experiments, substantial numbers of BCG were found in both the spleens and livers (Fig. 1). In livers, BCG was gradually eliminated and almost undetectable 40 weeks after vaccination. By contrast, bacterial numbers were unchanged from 2 to 40 weeks after vaccination in spleens.

We next examined the efficacy of BCG vaccination at 20 and 40 weeks postvaccination. Mice were challenged intratracheally with KM-resistant BCG. After 5 weeks, mice were sacrificed and CFUs of KM-resistant BCG in the lungs determined. We found that reduced numbers of CFUs in BCG-vaccinated mice comparing to that in unvaccinated mice at 20 weeks postvaccination. However, we could not find a reduction in CFUs in vaccinated mice at 40 weeks postvaccination (Fig. 2). The protective efficacy of BCG was evident 20 weeks after the vaccination but was lost at 40 weeks

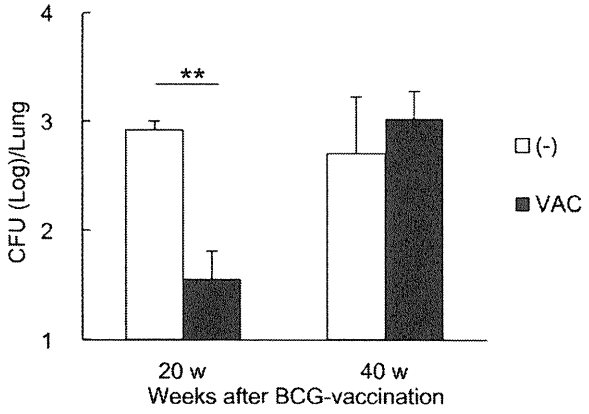

Fig. 2. Influence of time after vaccination on BCG-induced protection in C57BL/6 mice. Twenty or 40 weeks after BCG vaccination, C57BL/6 mice vaccinated with BCG (closed columns) or not (open columns) were intratracheally challenged with 5×10^4 of KM resistant BCG. Five weeks later, mice were sacrificed and CFUs of KM resistant BCG in lungs were counted. $^{**}P < 0.01$ versus unvaccinated mice. Data represent mean values ± SD for 4–6 mice per group.

after vaccination. The experiments were repeated twice, and the loss of protection at 40 weeks postvaccination was reproducibly observed (data not shown).

In order to know the precise mechanism of BCG efficacy, we examined helper T (TH) cell cytokine patterns. TH1 immune responses, such as the production of IFN-gamma, are protective against mycobacterial infection, whereas type 2 helper T cell (TH2) responses, such as production of IL-4 and IL-5, are not [17,18]. To clarify the mechanism of BCG efficacy, we examined cytokine responses of lymph node cells against *M. tuberculosis* antigens, PPD, at 20 and 40 weeks postvaccination. High levels of IFN-gamma production were observed when lymph node cells derived from mice 20, but not 40, weeks after vaccination were incubated with PPD (Fig. 3A). By contrast, significant production of both IL-4 and IL-5 was observed when lymph node cells derived from mice at 40 weeks postvaccination were incubated with PPD (Fig. 3B and C).

3.2. BCG induces protection in aged mice

In order to clarify the participation of age factors in the decline of protection induced by BCG vaccination, we studied BCG efficacy using aged mice. Young (5 weeks old) and aged (45–55 weeks old) C57BL/6 mice were intraperitoneally vaccinated with 10^5 CFUs of BCG. Mice were then challenged with KM-resistant BCG and protection was assessed by comparing CFUs of KM-resistant BCG in the lungs at 5 weeks postchallenge (Fig. 4A). Significantly reduced numbers of CFUs were seen in both BCG-vaccinated young and aged mice comparing to unvaccinated controls, showing that BCG vaccination can induce protection in mice aged 45–55 weeks. Simultaneously, we studied cytokine responses of lymph node cells. Lymph node cells derived from aged mice prevaccinated with BCG produced comparable amounts of IFN-gamma to young mice, when stimulated with PPD (Fig. 4B). The $CD4^+$ splenic T cells produced similar levels of IFN-gamma when stimulated with PPD as lymph node cells (data not shown).

3.3. Protection is lost despite maintenance of TH1 responses to PPD

We next examined whether the loss of BCG effectiveness observed in C57BL/6 mice occurred in another mouse strain, BALB/c. In C57BL/6 mice, we observed impaired TH1 and strengthened TH2 responses of lymph node cells to PPD when protection was diminished (Fig. 3). We considered this shift of immune

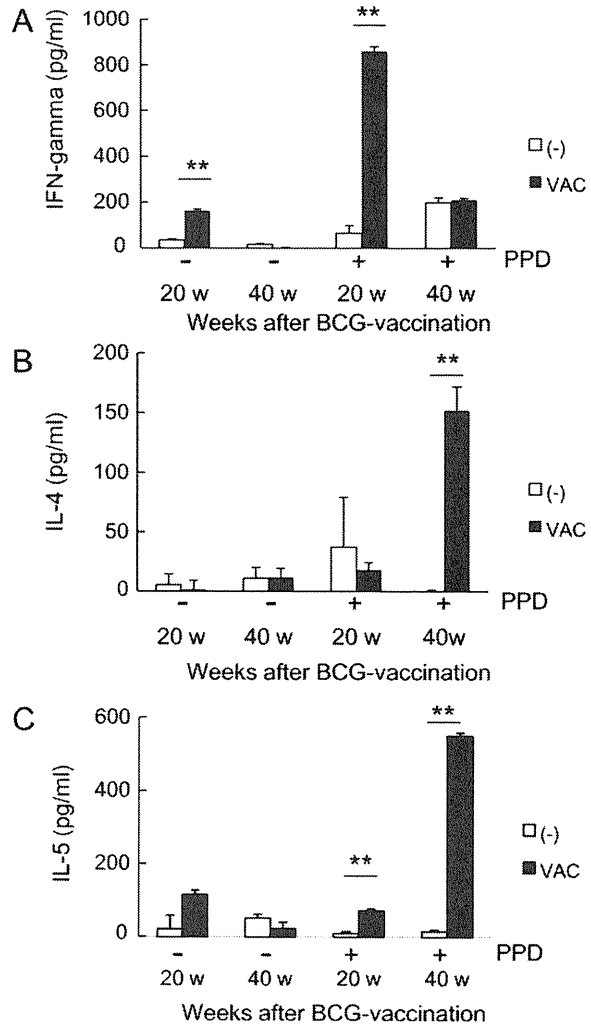

Fig. 3. Cytokine production from lymph node cells after stimulation with *M. tuberculosis* antigens, PPD *in vitro*. Lymph nodes cells (2.5×10^6 cells/ml) derived from BCG-vaccinated (closed columns) or unvaccinated (open columns) mice were cultured with or without 10 μg/ml of PPD for 7 days. The amounts of IFN-gamma (A), IL-4 (B), and IL-5 (C) in the supernatants were determined by ELISA. $^{*}P < 0.05$, $^{**}P < 0.01$ versus unvaccinated mice.

response from TH1 to TH2 to mycobacterial antigens might cause loss of protection. To examine this hypothesis as well, we used STAT6 deficient BALB/c mice previously constructed [19]. STAT6 is a transcription factor that translocates to the cell nucleus after phosphorylation and plays a central role in IL-4 mediated biological function [20,21]. Robust TH1 and impaired TH2 responses are reported in STAT6 knockout mice [20,21].

Wild-type BALB/c and STAT6 knockout mice were vaccinated with 10^5 CFU BCG intraperitoneally and viable numbers of BCG in spleens and liver were counted (Fig. 5A and B). In spleens, 10^4–10^5 CFUs of BCG continuously remained in both wild type and STAT6 knockout BALB/c mice until 40 weeks after vaccination (Fig. 5A). As observed in C57BL/6 mice, both mice showed a gradual decrease of inoculated BCG in the liver (Fig. 5B).

We next examined TH1 responses to PPD in STAT6 knockout mice after BCG vaccination. Twenty and 40 weeks after vaccination, we analyzed the responses of lymph node cells (Fig. 6) and $CD4^+$ T cells to PPD *in vitro*. T cells of STAT6-knockout mice showed significantly higher levels of proliferation when compared to control mice at both 20 and 40 weeks postvaccination (Fig. 6A). Significantly higher levels of IFN-gamma production were detected from lymph node cells of STAT6 knockout mice compared to wild type

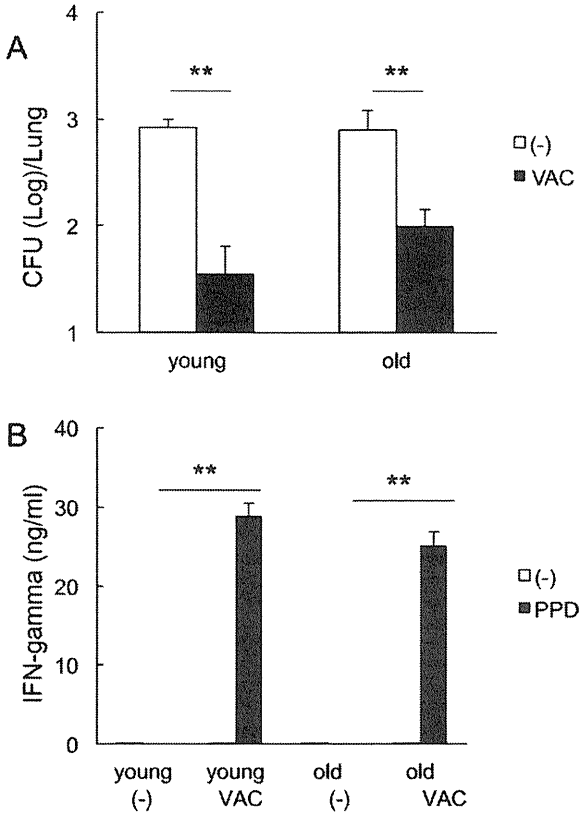

Fig. 4. Effect of BCG vaccination in aged C57BL/6 mice. Young (5 weeks old) and aged (45–55 weeks olds) mice were vaccinated with BCG. Five weeks after vaccination, mice were intratracheally challenged with KM resistant BCG and sacrificed at 5 weeks postchallenge. Living bacterial numbers in vaccinated (closed column) or unvaccinated (open column) mouse lungs were counted (A). Five weeks after vaccination, 2.5×10^6 lymph node cells were cultured with (closed columns) or without (open columns) of 10 μg/ml of PPD for 7 days. The levels of IFN-gamma in culture supernatants were determined by ELISA (B). Data represent mean values ± SD for 6 mice per group in (A). $^{**}P < 0.01$ versus unvaccinated mice in both (A) and (B).

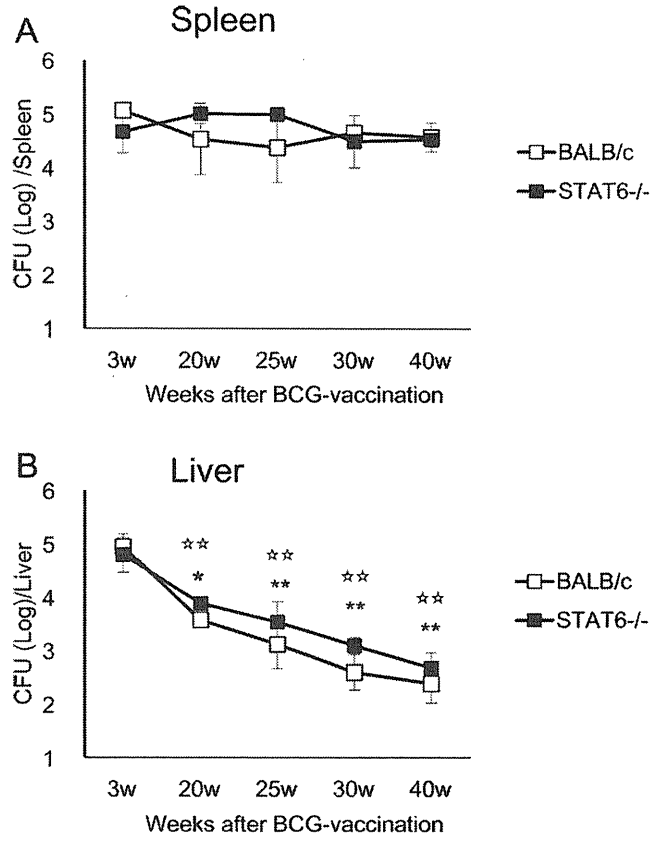

Fig. 5. Survival of BCG in BALB/c and STAT6 knockout mice after vaccination. BALB/c and STAT6 knockout mice were intraperitoneally vaccinated with 10^5 CFU of BCG. At various times after vaccination, bacterial numbers in the spleen (A) and liver (B) of BALB/c (open squares) or STAT6 knockout (closed squares) mice were counted after plating serially diluted lung homogenates on 7H11-OADC agar. Data represent mean values ± SD for 4–5 mice per group. $^{☆☆}P < 0.01$ versus CFU of BALB/c mice at 3 weeks after vaccination. $^{**}P < 0.01$; $^{*}P < 0.05$ versus CFU of STAT 6 knockout mice at 3 weeks after vaccination.

mice at both 20 and 40 weeks postvaccination (Fig. 6B). The reduction of IFN-gamma responses to PPD observed in wild type C57BL/6 (Fig. 3A) at 40 weeks after infection was not seen in STAT6 knockout mice or wild type mice (Fig. 6B). We obtained similar results when using splenic $CD4^+$ T cells and APCs (data not shown).

Simultaneously, we analyzed TH2 cytokine production in cultured supernatants. We could detect IL-4 production from lymph node cells when those were stimulated with PPD at both time points. The level of IL-4 was significantly lower in STAT6 knockout than wild type mice at both time points (Fig. 6C). By contrast, small amount of IL-5 production (213 ± 6.5 pg/ml) was seen when lymph node cells derived from wild type but not STAT6 knockout mice at 20 weeks after vaccination (data not shown). Lymph node cells derived from neither wild type nor STAT6 knockout mice at 40 weeks after vaccination produced IL-5 upon stimulated with PPD (data not shown). Taken together, in BALB/c mice, the TH1 immune response to PPD was maintained and in STAT6 knockout mice, the TH1 polarized immune response was maintained until 40 weeks postvaccination.

Finally we addressed whether the protective effects of BCG vaccination is maintained in TH1 polarized STAT6 knockout mice. Mice vaccinated with BCG or given saline were intratracheally challenged with KM-resistant BCG at 3, 20 and 40 weeks postvaccination. We accessed the protective effects by comparing CFUs of KM-resistant BCG in the lungs (Fig. 7). We found significantly reduced CFUs in BCG-vaccinated mice compared to unvaccinated mice at both 3 and 20 weeks postvaccination (Fig. 7A and B). As seen in the experiments using C57BL/6 mice, impairment of protection was seen in BALB/c mice at 40 weeks postvaccination (Fig. 7C). We also found loss of the protective effects of BCG vaccination in STAT6 knockout mice 40 weeks after vaccination (Fig. 7C).

4. Discussion

Poor effectiveness of the BCG vaccine is a serious matter in controlling tuberculosis [3]. There is an urgent demand to develop novel vaccination strategies or vaccines against tuberculosis. In order to understand the mechanism behind the poor effectiveness of BCG and to evaluate novel vaccine candidates, animal models are critically useful. However, it was thought that BCG vaccination provides good protection from mycobacterial infection in animal models. Accordingly, the usefulness of animal models for developing tuberculosis vaccines has been questioned, because they do not seem to reflect poor protective efficacy of BCG against adult pulmonary tuberculosis. In this study, we showed that efficacy of BCG is lost over time following vaccination in both C57BL/6 and BALB/c mice (Figs. 2 and 7). In these mice adaptive immunity differently respond to some intracellular pathogens such as *Leishmania* and *Yersinia* [22,23]. In such infections, C57BL/6 mice mount strong TH1-type responses, whereas BALB/c mice preferentially activate TH2-type responses, leading different infectious outcomes [22,23]. In contrast, TH1 type immune responses similarly occur in mycobacterial infection in both mouse strains, although C57BL/6

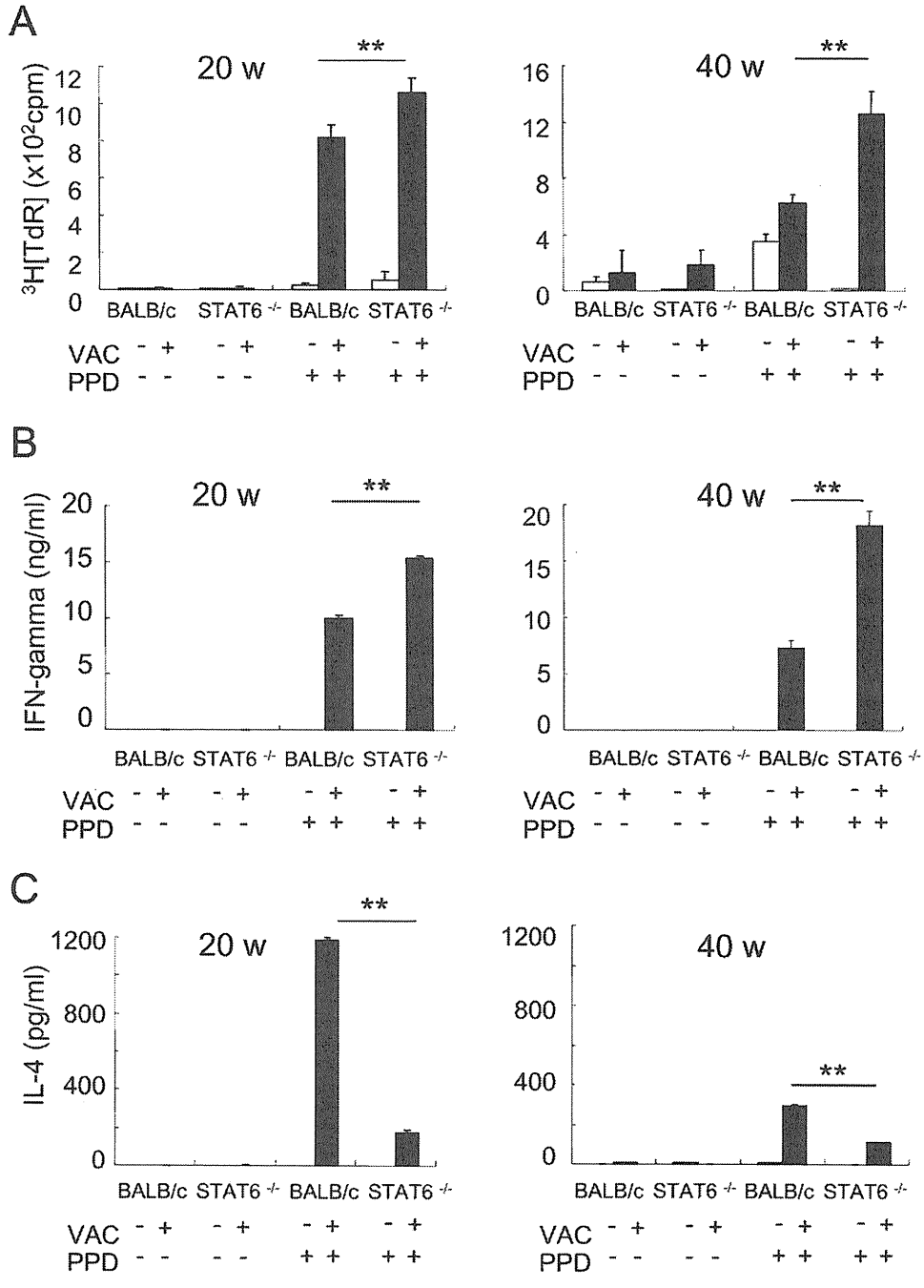

Fig. 6. Immune responses of lymph node cells derived from BALB/c and STAT6 knockout mice after stimulation with PPD. 2.5×10^6 lymph node cells were cultured with or without 10 μg/ml of PPD for 5 days. Uptake of ^{3}H labeled thymidine was determined (A). The amounts of IFN-gamma (B) and IL-4 (C) in the culture supernatants were determined by ELISA. Black columns, vaccinated BALB/c or STAT6 knockout mice. White columns, unvaccinated BALB/c and STAT6 knockout mice. $^{**}P < 0.01$ vaccinated BALB/c mice versus vaccinated STAT6 mice.

relatively TH1-prone than BALB/c mice [24], and resist equally against *M. tuberculosis* challenge [25,26].

In this study, the loss of protection was not dependent on the elimination of vaccinated BCG in the animals (Figs. 1 and 5) or advanced age of the mice (Fig. 4). Ito et al. reported that even 24-month old mice can be protected by BCG vaccination to a comparable level as young mice [27]. BCG also induced similar protection in old (60 month old) and middle aged guinea pigs as compared with young guinea pigs [28]. Thus BCG is likely to induce protection for a certain period of time after vaccination, but our study shows its efficacy is eventually lost over time following vaccination in mouse models.

The decline of BCG efficacy was reported in the human studies. One study enrolled 54,239 persons in England showed the efficacy of BCG within the first 5 years are 84% but it was gradually decreased to 59% after 15 years [8]. Another study performed in the United States enrolled 64,136 persons, also reported rapid loss of BCG efficacy 4 years after vaccination [9]. From these reports, it would be probably reasonable to consider that loss of protection occurred in BCG-vaccinated human with time. However one report showed that efficacy maintained over 50 years by the survey of relatively small (2792) number of subjects. Our finding prompts the requirement for the exact survey of the duration of effectiveness of BCG in adult human beings.

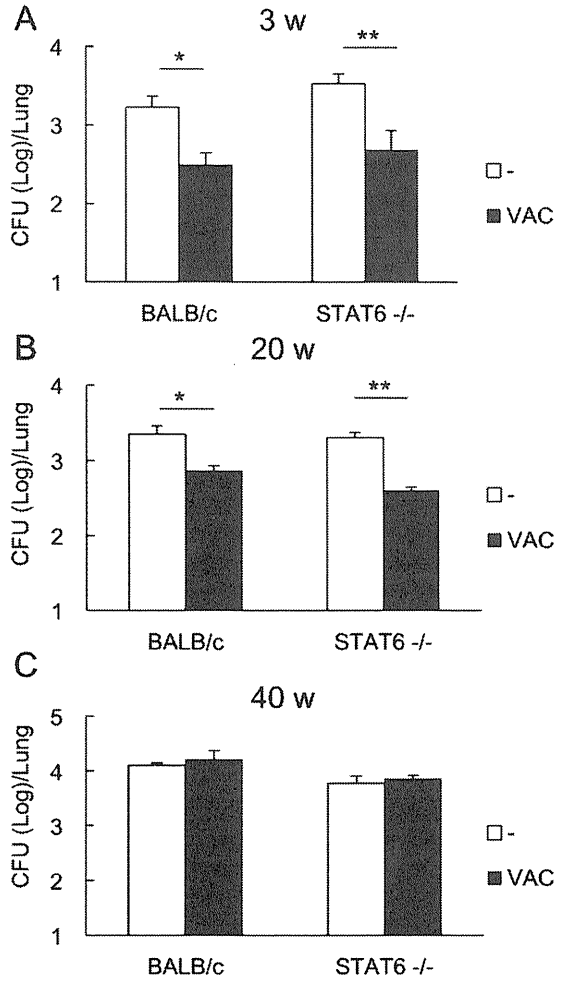

Fig. 7. Influence of time on BCG-induced protection in BALB/c and STAT6 knockout mice. Three, 20, and 40 weeks after BCG vaccination, BCG-vaccinated BALB/c and STAT6 knockout (black columns), unvaccinated BALB/c and STAT6 knockout mice (white columns) were challenged with 10^5–10^6 CFU of KM resistant BCG intratracheally. Five weeks later, mice were sacrificed and CFUs of KM resistant BCG in lungs were determined. $^{**}P<0.01$; $^{*}P<0.05$ versus unvaccinated mice.

If the mice model established in this study would reflect variable or low protectiveness of BCG vaccination against adult pulmonary tuberculosis, this model would be useful in the analysis of immune responses and evaluation of newly developed vaccines. Currently, prime-booster vaccination is one of the viable vaccination strategies [18]. This loss of BCG efficacy mouse model is useful for studying the regeneration of protectiveness after boosting with new vaccine candidates.

Sakai et al. recently reported a reduction in efficacy 12 weeks after BCG vaccination in mice [29]. They found a reduction in programmed cell death ligand 1 (PD-L1) expression on the antigen-expressing cell 3 weeks after BCG vaccination and programmed cell death 1 (PD-1) knockout mice acquired stronger protection following BCG vaccination. Because the PD-1-PD-L1 pathway negatively regulates antigen receptor signaling between T cells and APCs [30], they concluded that the PD-1-PD-L1 pathway-dependent impairment of TH1 immunity is involved in the reduction in BCG-induced protection. We also observed a reduction in TH1 immune responses to PPD in C57BL/6 mice (Fig. 3A) although this was still evident in BALB/c mice (Fig. 6B). In addition, analysis of BALB/c and STAT-6 knockout mice showed that the protectiveness of the BCG vaccination was lost despite the maintenance of TH1 immune responses to *M. tuberculosis* antigens (Figs. 6 and 7). Although activation of the PD-1-PD-L1 pathway participates in a reduction of TH1 immunity upon BCG vaccination [29], our results suggest that the reduction of TH1 immune responses does not fully explain the loss of BCG-induced protection.

Although responses of lymph node cells and splenic $CD4^+$ cells to *M. tuberculosis* antigens are different between C57BL/6 (Fig. 3) and BALB/c (Fig. 6) mice, both mice similarly lost protectiveness of BCG at 40 weeks post vaccination, implying that an unknown common mechanism caused loss of effectiveness in both mice. IFN-gamma plays a central role in acquired protective immunity against tuberculosis in both mice [11,13,31] and humans [14,15]. However solely detecting the production of IFN-gamma is not a sufficient biomarker to predict protective status from tuberculosis [32] and Scanga et al. reported reactivation of persistent tuberculosis despite continued expression of interferon gamma in mice [33]. Loss of protectiveness of the BCG vaccination in spite of maintenance of the IFN-gamma productivity of T cells following stimulation with PPD (Figs. 6 and 7) suggests that it might be due to unresponsiveness to IFN-gamma signaling or some unknown mechanism separated from IFN-gamma signaling. One possible mechanism is regulatory T cells (Tregs). However, Sakai et al. predicted a minor contribution of Tregs in the reduction of BCG-induced protectiveness [29] and we and other groups suggested minor roles for Tregs in mycobacteria infection [34–36], although others have reported the contribution of Tregs in immune suppression in mycobacterial infection [37,38]. In our preliminary experiments, robust IL-10 production was observed from lymph node cells and purified $CD4^+$ cells derived from mice after 40 weeks vaccination following PPD stimulation (our unpublished data). Since IL-10 is an immunosuppressive cytokine, it may be one of the possible factors involved in loss of BCG-induced protection. In order to clarify the mechanism of reduced protection and the possible roles of immunosuppressive cytokines and cells, mice that had received the BCG vaccination a long time ago should be used in future studies.

5. Conclusion

This study shows that a reduction in efficacy of the BCG vaccination against mycobacterial infection occurs in mice over time following vaccination. The duration from vaccination should be considered when assessing the variation of BCG efficacy against adult pulmonary tuberculosis. This mouse model demonstrating the loss of BCG effectiveness should be useful for understanding the BCG vaccine and aid the development effective tuberculosis vaccines.

Acknowledgments

This work was supported by grants from the Ministry of Education Culture Sports Science and Technology, Ministry of Health, Labour and Welfare (Research on Emerging and Re-emerging Infectious Diseases, Health Sciences Research Grants), The Japan Health Sciences Foundation (to Y.O., T.T., S.Y., K.K., and S.M.). We also thank Sara Matsumoto for assistance with the experiments and heartfelt encouragement.

References

[1] WHO. http://www.who.int/tb/publications/global_report/2009/update/en/index.html; 2010.
[2] WHO. BCG: bad news from India. Lancet 1980;1(8159):73–4.
[3] Fine PE. Variation in protection by BCG: implications of and for heterologous immunity. Lancet 1995;346(8986):1339–45.
[4] Colditz GA, Brewer TF, Berkey CS, Wilson ME, Burdick E, Fineberg HV, et al. Efficacy of BCG vaccine in the prevention of tuberculosis. Meta-analysis of the published literature. JAMA 1994;271(9):698–702.
[5] Behr MA, Wilson MA, Gill WP, Salamon H, Schoolnik GK, Rane S, et al. Comparative genomics of BCG vaccines by whole-genome DNA microarray. Science 1999;284(5419):1520–3.

[6] Brandt L, Feino Cunha J, Weinreich Olsen A, Chilima B, Hirsch P, Appelberg R, et al. Failure of the *Mycobacterium bovis* BCG vaccine: some species of environmental mycobacteria block multiplication of BCG and induction of protective immunity to tuberculosis. Infect Immun 2002;70(2):672–8.
[7] Clemens JD, Chuong JJ, Feinstein AR. The BCG controversy. A methodological and statistical reappraisal. JAMA 1983;249(17):2362–9.
[8] Comstock GW, Palmer CE. Long-term results of BCG vaccination in the southern United States. Am Rev Respir Dis 1966;93(February (2)):171–83.
[9] Hart PD, Sutherland I. BCG and vole bacillus vaccines in the prevention of tuberculosis in adolescence and early adult life. Br Med J 1977;2(July (6082)):293–5.
[10] Aronson NE, Santosham M, Comstock GW, Howard RS, Moulton LH, Rhoades ER, et al. Long-term efficacy of BCG vaccine in American Indians and Alaska Natives: a 60-year follow-up study. JAMA 2004;291(May (17)):2086–91.
[11] Kawamura I, Tsukada H, Yoshikawa H, Fujita M, Nomoto K, Mitsuyama M. IFN-gamma-producing ability as a possible marker for the protective T cells against *Mycobacterium bovis* BCG in mice. J Immunol 1992;148(9):2887–93.
[12] Cooper AM, Dalton DK, Stewart TA, Griffin JP, Russell DG, Orme IM. Disseminated tuberculosis in interferon gamma gene-disrupted mice. J Exp Med 1993;178(6):2243–7.
[13] Flynn JL, Chan J, Triebold KJ, Dalton DK, Stewart TA, Bloom BR. An essential role for interferon gamma in resistance to *Mycobacterium tuberculosis* infection. J Exp Med 1993;178(6):2249–54.
[14] Jouanguy E, Altare F, Lamhamedi S, Revy P, Emile JF, Newport M, et al. Interferon-gamma-receptor deficiency in an infant with fatal bacille Calmette-Guerin infection. N Engl J Med 1996;335(26):1956–61.
[15] Newport MJ, Huxley CM, Huston S, Hawrylowicz CM, Oostra BA, Williamson R, et al. A mutation in the interferon-gamma-receptor gene and susceptibility to mycobacterial infection. N Engl J Med 1996;335(26):1941–9.
[16] Orme IM. Induction of nonspecific acquired resistance and delayed-type hypersensitivity, but not specific acquired resistance in mice inoculated with killed mycobacterial vaccines. Infect Immun 1988;56(12):3310–2.
[17] Flynn JL, Chan J. Immunology of tuberculosis. Annu Rev Immunol 2001;19:93–129.
[18] Young DB, Perkins MD, Duncan K, Barry 3rd CE. Confronting the scientific obstacles to global control of tuberculosis. J Clin Invest 2008;118(4):1255–65.
[19] Kaplan MH, Schindler U, Smiley ST, Grusby MJ. Stat6 is required for mediating responses to IL-4 and for development of Th2 cells. Immunity 1996;4(3):313–9.
[20] Shimoda K, van Deursen J, Sangster MY, Sarawar SR, Carson RT, Tripp RA, et al. Lack of IL-4-induced Th2 response and IgE class switching in mice with disrupted Stat6 gene. Nature 1996;380(6575):630–3.
[21] Takeda K, Tanaka T, Shi W, Matsumoto M, Minami M, Kashiwamura S, et al. Essential role of Stat6 in IL-4 signalling. Nature 1996;380(6575):627–30.
[22] Heinzel FP, Sadick MD, Holaday BJ, Coffman RL, Locksley RM. Reciprocal expression of interferon gamma or interleukin 4 during the resolution or progression of murine leishmaniasis. Evidence for expansion of distinct helper T cell subsets. J Exp Med 1989;169(January (1)):59–72.
[23] Bohn E, Heesemann J, Ehlers S, Autenrieth IB. Early gamma interferon mRNA expression is associated with resistance of mice against *Yersinia enterocolitica*. Infect Immun 1994;62(July (7)):3027–32.
[24] Wakeham J, Wang J, Xing Z. Genetically determined disparate innate and adaptive cell-mediated immune responses to pulmonary *Mycobacterium bovis* BCG infection in C57BL/6 and BALB/c mice. Infect Immun 2000 Dec;68(12):6946–53.
[25] Chackerian AA, Behar SM. Susceptibility to *Mycobacterium tuberculosis*: lessons from inbred strains of mice. Tuberculosis (Edinb) 2003;83(5):279–85.
[26] Jung YJ, Ryan L, LaCourse R, North RJ. Differences in the ability to generate type 1T helper cells need not determine differences in the ability to resist *Mycobacterium tuberculosis* infection among mouse strains. J Infect Dis 2009;199(June (12)):1790–6.
[27] Ito T, Takii T, Maruyama M, Hayashi D, Wako T, Asai A, et al. Effectiveness of BCG vaccination to aged mice. Immun Ageing 2010;7:12.
[28] Komine-Aizawa S, Yamazaki T, Yamazaki T, Hattori S, Miyamoto Y, Yamamoto N, et al. Influence of advanced age on *Mycobacterium bovis* BCG vaccination in guinea pigs aerogenically infected with *Mycobacterium tuberculosis*. Clin Vaccine Immunol 2010;17(10):1500–6.
[29] Sakai S, Kawamura I, Okazaki T, Tsuchiya K, Uchiyama R, Mitsuyama M. PD-1-PD-L1 pathway impairs T(h)1 immune response in the late stage of infection with *Mycobacterium bovis* bacillus Calmette-Guerin. Int Immunol 2010;22(12):915–25.
[30] Okazaki T, Honjo T. PD-1 and PD-1 ligands: from discovery to clinical application. Int Immunol 2007;19(7):813–24.
[31] Orme IM, Roberts AD, Griffin JP, Abrams JS. Cytokine secretion by CD4 T lymphocytes acquired in response to *Mycobacterium tuberculosis* infection. J Immunol 1993;151(1):518–25.
[32] Parida SK, Kaufmann SH. The quest for biomarkers in tuberculosis. Drug Discov Today 2010;15(3–4):148–57.
[33] Scanga CA, Mohan VP, Yu K, Joseph H, Tanaka K, Chan J, et al. Depletion of CD4(+) T cells causes reactivation of murine persistent tuberculosis despite continued expression of interferon gamma and nitric oxide synthase 2. J Exp Med 2000;192(3):347–58.
[34] Ozeki Y, Sugawara I, Udagawa T, Aoki T, Osada-Oka M, Tateishi Y, et al. Transient role of CD4+CD25+ regulatory T cells in mycobacterial infection in mice. Int Immunol 2010;22(3):179–89.
[35] Quinn KM, McHugh RS, Rich FJ, Goldsack LM, de Lisle GW, Buddle BM, et al. Inactivation of CD4+ CD25+ regulatory T cells during early mycobacterial infection increases cytokine production but does not affect pathogen load. Immunol Cell Biol 2006;84(5):467–74.
[36] Quinn KM, Rich FJ, Goldsack LM, de Lisle GW, Buddle BM, Delahunt B, et al. Accelerating the secondary immune response by inactivating CD4(+)CD25(+) T regulatory cells prior to BCG vaccination does not enhance protection against tuberculosis. Eur J Immunol 2008;38(3):695–705.
[37] Kursar M, Koch M, Mittrucker HW, Nouailles G, Bonhagen K, Kamradt T, et al. Cutting edge: regulatory T cells prevent efficient clearance of *Mycobacterium tuberculosis*. J Immunol 2007;178(5):2661–5.
[38] Scott-Browne JP, Shafiani S, Tucker-Heard G, Ishida-Tsubota K, Fontenot JD, Rudensky AY, et al. Expansion and function of Foxp3-expressing T regulatory cells during tuberculosis. J Exp Med 2007;204(9):2159–69.

FEBS Letters 585 (2011) 2263–2268

FEBS Letters

journal homepage: www.FEBSLetters.org

Mitochondrial density contributes to the immune response of macrophages to lipopolysaccharide via the MAPK pathway

Emiko Kasahara [a,c,*,1], Atsuo Sekiyama [a,c,1], Mika Hori [a,1], Kenjiro Hara [a,1], Nozomi Takahashi [a,1], Masami Konishi [a,1], Eisuke F Sato [a,1], Sohkichi Matsumoto [b,1], Haruki Okamura [c,1], Masayasu Inoue [a,1]

[a] Department of Biochemistry and Molecular Pathology, Osaka City University Graduate School of Medicine, 1-4-3 Asahimachi, Abeno, Osaka 545-8585, Japan
[b] Department of Bacteriology, Osaka City University Graduate School of Medicine, 1-4-3 Asahimachi, Abeno, Osaka 545-8585, Japan
[c] Laboratory of Host Defenses, Institute for Advanced Medical Sciences, Hyogo College of Medicine, Nishinomiya, Hyogo, Japan

ARTICLE INFO

Article history:
Received 10 March 2011
Revised 8 May 2011
Accepted 20 May 2011
Available online 27 May 2011

Edited by Laszlo Nagy

Keywords:
Mitochondria
Innate immunity
Inflammatory cytokine
Macrophage
Reactive oxygen species
TLR4

ABSTRACT

We investigated the role of mitochondrial reactive oxygen species (ROS) in the response of macrophages to lipopolysaccharide (LPS) using RAW 264.7 cells and their ρ^0 cells lacking mitochondria. Mitochondrial density, respiratory activity and related proteins in ρ^0 cells were significantly lower than those in RAW cells. LPS rapidly stimulated mitochondrial ROS prior to cytokine secretion, such as TNF-α and IL-6, from RAW 264.7 cells by activating the MAPK pathway, while the response was attenuated in ρ^0 cells. Exposure of ρ^0 cells to H_2O_2 partially restored the secretion of cytokines induced by LPS. These results suggest that mitochondrial density and/or the respiratory state contribute to intracellular oxidative stress, which is responsible for the stimulation of LPS-induced MAPK signaling to enhance cytokine release from macrophages.

1. Introduction

Neutrophils and macrophages play important roles in the host defense mechanism against pathogens by producing reactive oxygen species (ROS), nitric oxide (NO) and cytokines. Stimulation of macrophages by a variety of microbial constituents including LPS is crucial for the following sequence of immune reactions. Toll-like receptors (TLRs) expressed on the surface membrane of macrophages and related immunocytes play important roles in antigen presentation and cytokine production by these cells [1–4]. TLR4 has been identified as a major sensor molecule for LPS of gram negative bacteria to mediate immune reactions. Exposure of macrophages to LPS triggers signaling pathway leading to activation of MAPK and NFκB to produce NO and inflammatory cytokines, such as TNF-α and IL-6 [5–7]. Although intracellular ROS has been postulated to underlie the mechanism of amplification of various signaling pathways [8,9], the source of ROS and the role of mitochondria have not been fully elucidated in innate immunity. Under physiological conditions, significant fractions of the inspired oxygen are converted to superoxide radical and related ROS [10]. Recent studies revealed that suppression of oxidative phosphorylation by down-regulating uncoupling proteins increased mitochondrial ROS generation and subsequently enhanced immunoreaction of LPS-treated macrophages [11,12], suggesting that mitochondrial respiratory status is important for the innate immune system. In general, total activity of mitochondrial respiration in the cell is correlated with the mitochondrial density. Furthermore, mitochondrial density has been shown to regulate intracellular ROS generation and determines the sensitivity of various cells to a variety of agents that induce mitochondria-dependent apoptosis [13]. These observations suggest that mitochondrial density could be one of the critical factors that determine the cellular response to various stimulants that activate signaling pathway leading to mitochondria-dependent oxidative stress. Thus, we hypothesized that mitochondrial density in LPS-treated macrophage contributes to

Abbreviations: ERK, extracellular signal-regulated kinase; LPS, lipopolysaccharide; MAPK, mitogen-activated protein kinase; MEK, MAPK-ERK kinase; NOx, nitric oxide metabolite; TNF-α, tumor necrosis factor-alpha; ROS, reactive oxygen species; TLR, Toll-like receptor; ρ^0 cell, cell lacking mitochondrial DNA; JNK, c-Jun-N-terminal kinase; NFκB, nuclear factor-kappa B; UCP2, uncoupling protein 2; MCF, Mean channel fluorescence; IκB, inhibitor of kappa B

* Corresponding author at: Department of Biochemistry and Molecular Pathology, Osaka City University Graduate School of Medicine, 1-4-3 Asahimachi, Abeno, Osaka 545-8585, Japan. Fax: +81 6 6645 3721.

E-mail address: kasahara@med.osaka-cu.ac.jp (E. Kasahara).

[1] E.K. and A.S. designed and conducted this study. E.K., A.S., M.H., K.H., N.T. and M.K. executed experiments. S.M., E.F.S. and M.I. contributed to this study with their critical discussion and suggestion. E.K., A.S. and M.I interpreted experiments and wrote the paper.

0014-5793/$36.00 © 2011 Federation of European Biochemical Societies. Published by Elsevier B.V. All rights reserved.
doi:10.1016/j.febslet.2011.05.049

the immune response by regulating ROS-accelerated signaling pathways. The present work describes the role of mitochondrial ROS in the enhancement of LPS-induced innate immune reactions using ρ^0 macrophages lacking mitochondrial DNA.

2. Materials and methods

2.1. Cell culture

Macrophage RAW 264.7 cells were cultured in RPMI1640 with 10 % heat-inactivated fetal bovine serum containing antibiotics (Nacalai Tesque, kyoto, Japan) at 37 °C in 5% CO_2. ρ^0 cells were established through long-term treatment of RAW cells with ethidium bromide (45 ng/ml) as described previously [14]. Prior to LPS (*Escherichia coli* O55 Sigma–Aldrich, St. Louis, MO) treatment, cells were plated in 24 well culture plates at a density of 10^5 cells/well and cultured for 24 h in the absence of ethidium bromide.

2.2. Levels of cytokines and nitric oxide metabolite (NO_x) in the culture medium

After 24 h incubation of the cells in the absence of ethidium bromide, LPS was added to give a final concentration of 1 μg/ml. Concentrations of cytokines and NO_x in the medium were determined using ELISA kits (eBioscience Inc., San Diego, CA) and NO_2/NO_3 Griess reagent kit (DOJINDO Lab., Kumamoto, Japan), respectively, according to the manufacture's instruction.

2.3. FACS analysis

After treatment with LPS, the cells were collected by trypsinization and analyzed by flow cytometry (FACS Calibuur, Becton Dickinson, San Jose, CA). Intracellular and mitochondrial ROS generation was detected using DHE and MitoSox Red (Invitrogen, Carlsbad, CA), respectively, according to the manufacture's protocols. Apoptosis was determined by Annexin V staining (MBL, Nagoya, Japan) and expression of TLR4 in cell surface was detected by incubation with anti-TLR4 antibody (eBioscience Inc.).

2.4. Confocal fluorescence microscopy

Cells were cultured on EZView culture plate (ASAHI GLASS, Tokyo, Japan) and mitochondrial contents and mitochondrial ROS generation were detected by staining with MitoTracker (Deep Red and Green FM) and MitoSox Red, respectively, according to the manufacture's protocols. Confocal fluorescence images were obtained using confocal microscope (Leica Microsystems, Wetzlar, Germany).

2.5. Western blotting

Cultured cells were collected by trypsinization, washed twice with ice-cold PBS and resuspended in a lysis buffer containing protease inhibitor cocktail (Nacalai Tesque). The lysed cell samples were subjected to SDS–PAGE and the protein bands were transferred to a Millipore Immobilon membrane (Waltham, MA) and subjected to immunoblot analysis using anti-TLR4 (sc-6525; Santa Cruz Biotechnology, Santa Cruz, CA), anti-phospho MAPK family (#9910; Cell Signaling Technology, Danvers, MA), anti-IκB-α (#9242; Cell Signaling Technology), and anti-mitochondrial complex antibodies (458099; Invitrogen, Carlsbad, CA). Immunoreactive bands were visualized using the enhanced chemiluminescence system (Immunostar; Wako Pure Chemical Co., Osaka, Japan), detected by a FujiFilm LAS-3000 camera and quantified using a FujiFilm Science Lab ImageGauge software.

2.6. Mitochondrial oxygen consumption

Cells were collected by trypsinization and resuspended in culture medium (10^7 cells/ml). Oxygen consumption was determined polarographically at 25 °C using a Clark-type oxygen electrode with 2 ml water-jacketed closed chamber.

2.7. Determination of NFκB and MAPK activity

Phosphorylated forms of NFκB (Ser536), P38 (Thr180/Tyr182), MEK1 (Ser217/221) and JNK (Thr183/Tyr185) were determined using PathScan Multi-Target Sandwich ELISA kit (Cell Signaling Technology, Danvers, MA) according to the manufacture's protocol, and the results were confirmed by western blotting method.

2.8. Statistical analysis

Values are expressed as the mean ± SE derived from 3-5 samples and the figures show the results obtained from three independent experiments. Statistical analysis was performed using analysis of variance (ANOVA) followed by Student's *t*-test and the level of significance was put at $P < 0.01$.

3. Results

3.1. Mitochondrial status and feature in RAW and their ρ^0 cell

To evaluate the role of mitochondrial function in the regulation of innate immunity and response of macrophages to LPS, we established their ρ^0 cells lacking mitochondrial DNA. As shown in Fig. 1A, mitochondrial density analyzed by the fluorescence intensity of MitoTracker Deep Red was significantly lower with ρ^0 cells than with RAW cells. Similar result was obtained by staining with MitoTracker Green, a probe that accumulates in the lipid environment of mitochondria independently of the membrane potential. The RAW cells cultured with ethidium bromide decreased mitochondrial density in a dose-dependent manner (Supplementary Fig. 1A). Mitochondrial respiratory activity and related proteins (complex I and IV) in ρ^0 cells were significantly lower than those in RAW cells (Fig. 1B and C). Despite the low density of mitochondria, ρ^0 cells grow as rapidly as RAW cells (Fig. 1D). Macrophages have been known to express TLR4 on their cell surface in poised to prime the responsiveness to the innate immune systems against pathogen. Cellular expression of TLR4 and their recruitment to cell surface in resting state occurred similarly with both RAW and their ρ^0 cells (Fig 2A and B).

3.2. LPS-stimulated ROS generation and cytokine secretion were low with ρ^0 cells

We investigated mitochondrial ROS generation in LPS-treated cells by MitoSox staining and analyzed using confocal fluorescence microscopy and FACS. Exposure of RAW cells to LPS for 24 h markedly increased intracellular (Fig. 3C) and mitochondrial (Fig. 3A and B) ROS while their responses were blunted in ρ^0 cells. Furthermore, mitochondrial generation of ROS was rapidly increased by LPS in prior to cytokine secretion and their intensities were significantly suppressed in ρ^0 cells (Fig. 3D). LPS stimulated the secretion of TNF-α and IL-6 more strongly with RAW cells than with ρ^0 cells (Fig. 3E and F). Furthermore, attenuation of TNF-α secretion in ρ^0 cells after LPS treatment appears to be occurred as a concomitant of mitochondrial loss (Supplementary Fig. 1B).

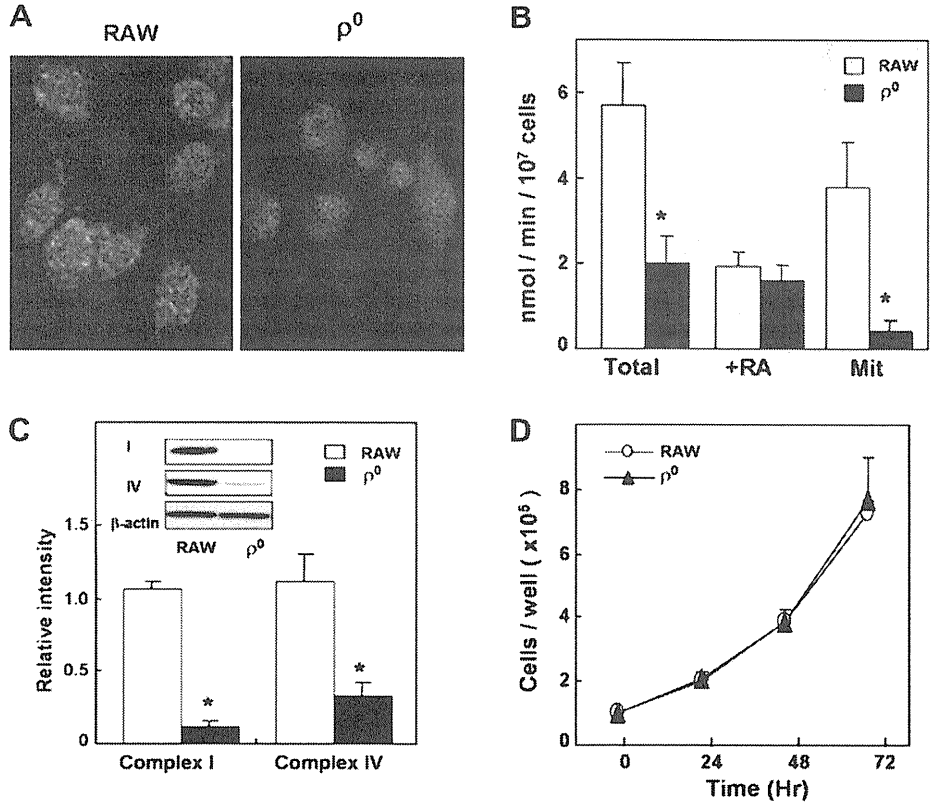

Fig. 1. Mitochondrial status and feature in RAW and ρ^0 cell. Mitochondrial status in RAW and ρ^0 cells was analyzed by mitochondrial staining with MitoTracker Deep Red (A). Mitochondrial density was confirmed by mitochondrial respiratory activity (B) and western blotting analysis for mitochondrial respiratory complex I and IV (C). Mitochondria-dependent oxygen consumption (Mit) was calculated by subtraction of oxygen consumption in the presence of rotenone and antimycin (+RA) from total oxygen consumption (B). Cell growth speed was measured by cell counting using hemocytometer (D). The data presented is representative of three independent experiments ($n = 3$, $^*P < 0.001$ vs RAW cell).

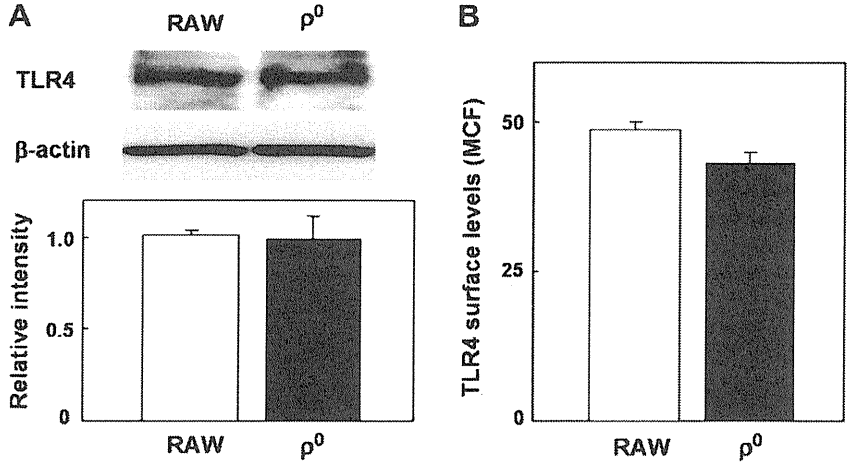

Fig. 2. Cellular expression and surface levels of TLR4 were similar in RAW and ρ^0 cell. Cellular TLR4 expression was analyzed by western blotting (A). Level of TLR4 on the plasma membrane was analyzed by FACScan systems (B). The data presented is representative of three independent experiments ($n = 3$).

3.3. LPS-stimulated NO generation and apoptosis were suppressed in ρ^0 cells

It has been well documented that LPS stimulates macrophages to generate nitric oxide and long time exposure to LPS induces their apoptosis. Thus, we analyzed the level of NO metabolite (NO_x) in the culture medium before and after stimulation by LPS in these cells (Fig. 4A). NO_x levels in culture medium were similar in WT and ρ^0 cells at basal level. Stimulation of macrophage with LPS for 24 h increased NO_x level in these cells, but was less in ρ^0 cell as compared with that in WT cells. After incubation with LPS for 48 h, significant fractions of the wild type macrophages underwent apoptosis (Fig. 4B). In contrast, apoptosis induced by LPS was not apparent in ρ^0 cells.

3.4. LPS-induced mitochondrial generation of ROS is involved in the enhancement of cytokine secretion

To test the possibility that mitochondrial ROS play critical roles in the enhancement of cytokine secretion, effect of various

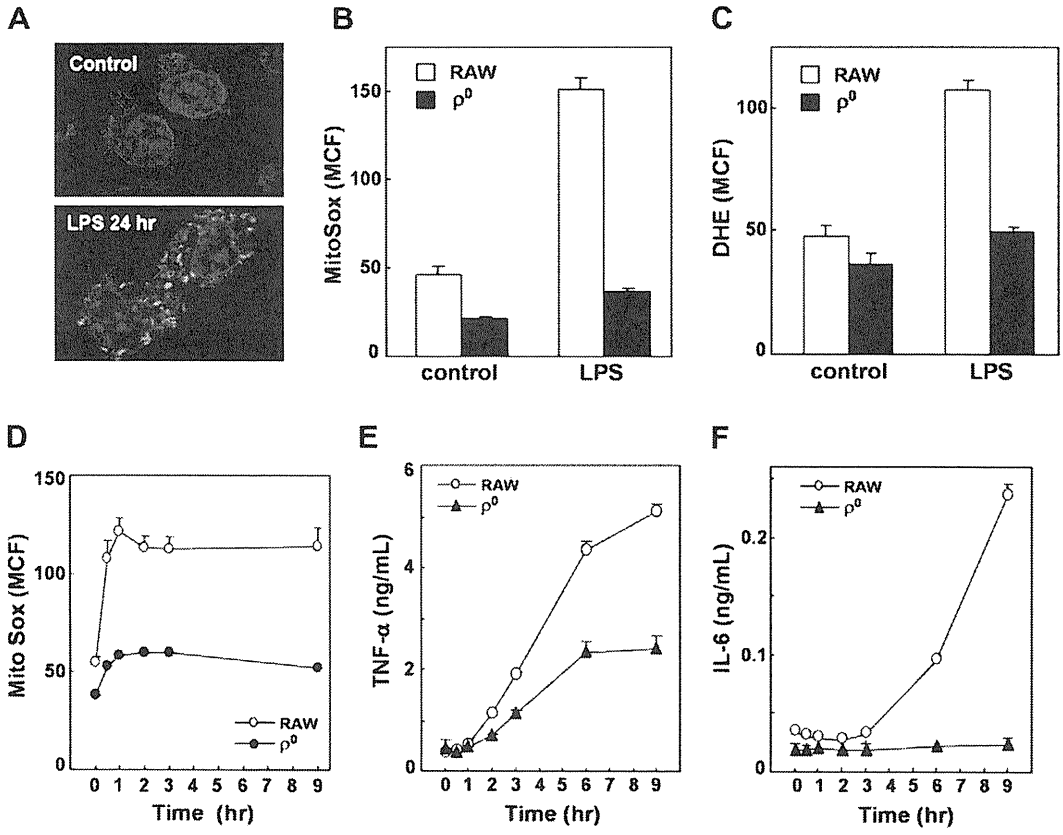

Fig. 3. LPS–stimulated ROS generation and the inflammatory cytokine secretion were reduced in ρ^0 cells. After treatment with LPS for 24 h, mitochondrial ROS generation were stained with MitoSox and observed under a confocal immunofluorescence microscopy (A). Intracellular (C) and mitochondrial (B) ROS generations in RAW and ρ^0 cells by LPS treatment for 24 h were determined by DHE and MitoSox Deep Red staining respectively and analyzed using FACScan systems. Time course of mitochondrial ROS generation (D) and secretion of TNF-α (E) and IL-6 (F) in response to LPS were detected as described in the text. The data presented is representative of three independent experiments.

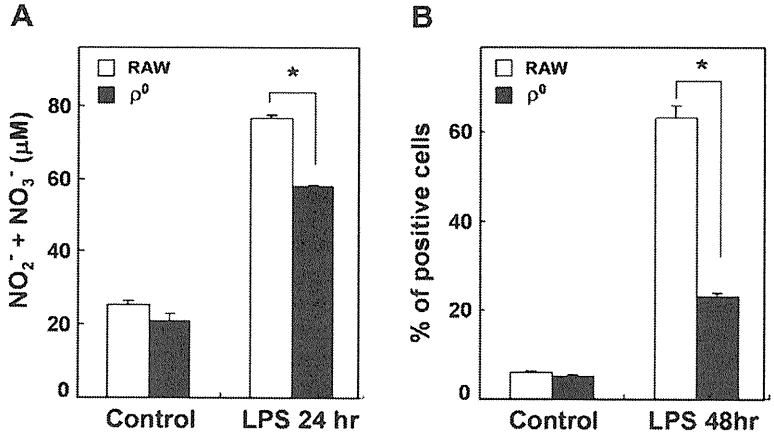

Fig. 4. NO_x production and apoptosis by LPS treatment were suppressed in ρ^0 cell. NO_x level in the medium 24 h after LPS treatment in WT and ρ^0 cells was measured as described in Section 2.2 (A). Apoptosis induced by LPS treatment for 48 h in WT and ρ^0 cells were measured by Annexin V staining and analyzed using FACScan systems. The data presented is representative of three independent experiments ($n = 5$, $^*P < 0.001$ vs RAW).

antioxidative agents on LPS-induced TNF-α secretion was investigated. The increased generation of mitochondrial ROS and secretion of TNF-α by LPS-treated macrophages were inhibited by the presence of N-acetyl cysteine but not SOD and apocynin, an inhibitor of NADPH oxidase (Fig. 5A and B). The LPS-induced TNF-α secretion was stimulated further with ρ^0 cells but not RAW cells after exposure to H_2O_2 generated by glucose (10 mM) and glucose oxidase (3 mU/ml).

3.5. Effect of LPS on the signaling pathways in RAW and ρ^0 cell

ROS has been shown to potentiate LPS-induced signaling pathways by activating transcriptional factors, such as NF-κB and MAPK family. Fig. 6 showed that LPS strongly activated NFκB, MEK-1, P38 MAPK and JNK in RAW cells. However, the LPS-induced activation was significantly low in ρ^0 cells except for NFκB. Similar results were obtained using western blotting method (Supplementary Fig. 2).

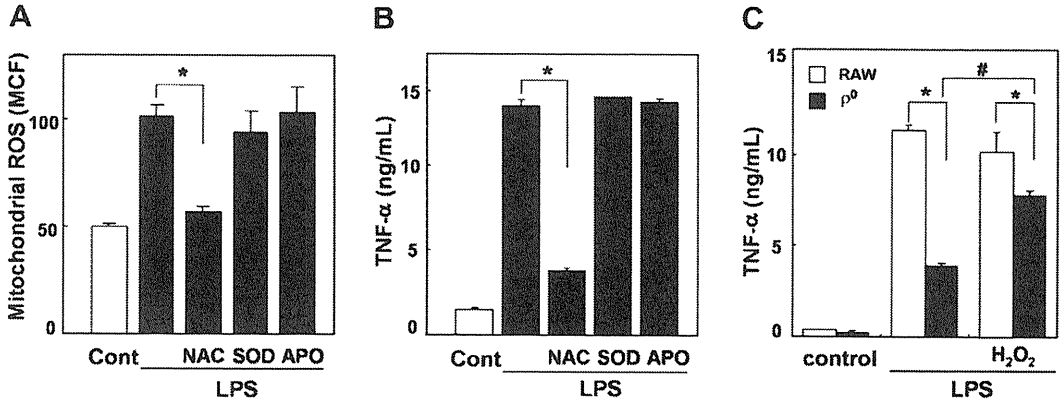

Fig. 5. Mitochondrial ROS generation by LPS is involved in the enhancement of cytokine secretion. Cells were preincubated with NAC, SOD and apocynin (APO) for 2 h and then exposure to LPS for 24 h. Mitochondrial generation of ROS (A) was analyzed using FACScan systems and TNF-α in the medium (B) was measured as described in the text. (C) RAW and their ρ^0 cell were incubated with LPS in the presence or absence of 10 mM glucose and 3 mU/ml glucose oxidase (GOX) and then TNF-α in the culture medium were measured. The data presented is representative of three independent experiments ($n = 3$, $^*P < 0.01$; $^{\#}P < 0.01$ vs RAW or LPS alone).

3.6. Effect of MAPK inhibitors on LPS-induced TNF-α secretion in RAW and ρ^0 cell

To know the possible involvement of MAPK signaling in response to LPS, we further attempted to determine the responsibility of mitochondria for TNF-α secretion in these cells using various specific inhibitors of MAPK. Fig. 7 showed that TNF-α secretion in response to LPS was significantly suppressed by pretreatment of RAW cells with the JNK inhibitor (SP600125) or the p38 inhibitor (SB202190), but not by the ERK inhibitor (PD98059). On the other hand, these MAPK inhibitors had no such effect with ρ^0 cells.

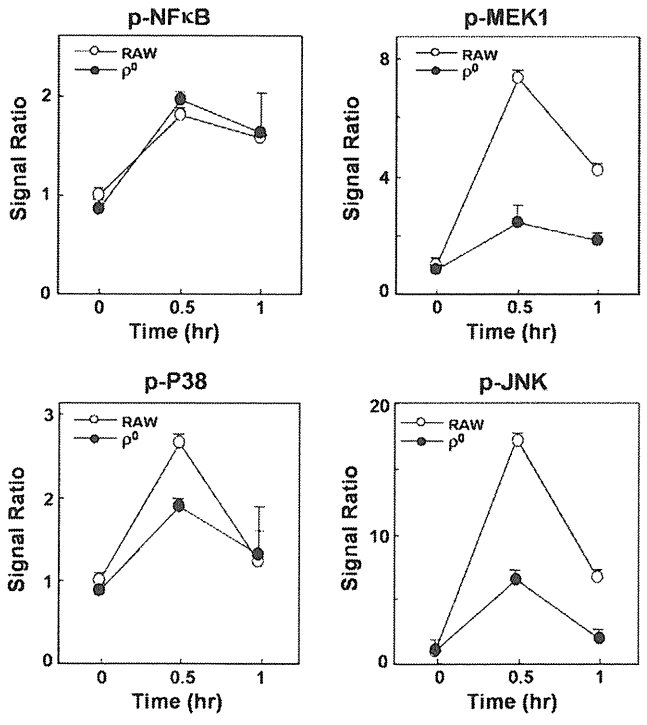

Fig. 6. LPS-induced MAPK activation was suppressed in ρ^0 cell. RAW and ρ^0 cells exposure to LPS for 0.5, 1 h or remain untreated (time 0) were collected and then the phosphorylation of NFκB, P38, MEK1 and JNK were measured as described in the text. Data were expressed as fold increase relative to the value observed in RAW cell that were not stimulated by LPS. Representative data of three independent experiments showing similar results are shown here. The data presented is representative of three independent experiments ($n = 3$).

4. Discussion

In this study, we demonstrated that mitochondrial generation of ROS is involved in the response of macrophage to LPS via MAPK pathway. Mitochondrial DNA-diminished ρ^0 cell showed lower mitochondrial density as compare with their wild type cells, and displayed reduced phenotype of LPS-induced ROS generation and MAPK phosphorylation thereby blunts the amplification of cytokine secretion.

Mitochondria play a crucial role in various cell metabolisms and function such as ATP production, ROS generation, and induction of apoptosis. ROS generation has been implicated in multiple physiological and pathological processes as a secondary messenger in cell signaling. Recently it has been reported that mitochondria might be a source of ROS generation in immune responses such as infection and inflammation [12,15]. Although biochemical process for inducing mitochondrial ROS generation in immune response is still under the debate, several reports revealed the physiological role of uncoupling protein 2 (UCP2) to regulate ROS generation in activated macrophages [16–18]. UCP2 a member of the anion carrier superfamily of mitochondrial inner membrane enhance the extent of mild uncoupling of the electrochemical gradient of mitochondria

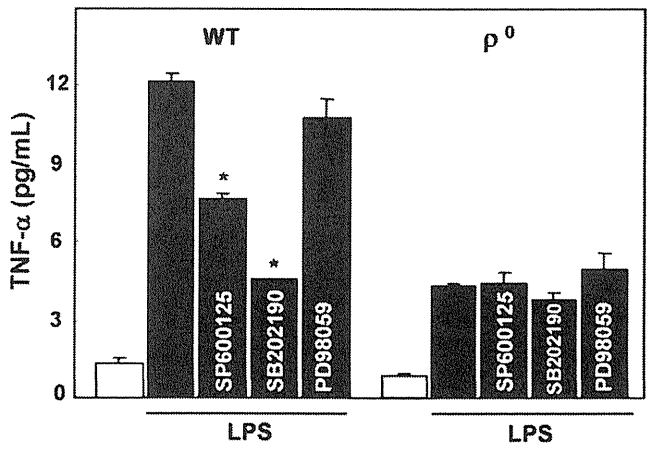

Fig. 7. Phosphorylation of P38 and JNK is involved in the mitochondria-dependent cytokine secretion. Cells were preincubated with 5 μM of JNK inhibitor (SP600125), p38 inhibitor (SB202190), and ERK inhibitor (PD98059) for 30 min and then exposure to LPS for 24 h. Secretion of TNF-α in response to LPS was detected as described in Section 2.2. The data presented is representative of three independent experiments. ($n = 3$, $^*P < 0.01$ vs LPS alone).

and observed to reduce generation of mitochondrial ROS. Recent study revealed that UCP2 is rapidly degraded by the cytosolic ubiquitin-proteasome system [19], and LPS-induced rapid degradation of UCP2 was necessary to increase mitochondrial ROS generation to activate MAPK pathway reading to cytokine secretion [11] [20]. In our study, mitochondria-diminished ρ^0 macrophage showed reduced ROS generation and MAPK phosphorylation in response to LPS treatment. On the other hand, LPS-induced NFκB activity is similarly upregulated in WT and ρ^0 cells. These evidences suggest that mitochondrial ROS generation has responsibility to enhance immune response via MAPK activation, and altered mitochondrial function such as activity of mitochondrial respiration and their density might affect the function of immune cells.

TLR4 is known to be a main sensor for LPS by triggering the pathway to produce inflammatory cytokines in macrophages [1–4]. And hence, LPS responsiveness is partly determined by the levels of TLR4 expression on cell surface and/or the function [21]. It has been reported that ROS modulate TLR4 signaling transduction partly by enhancing surface trafficking of TLR4 to lipid rafts in plasma membrane [22,23]. In the present study, cellular expression of TLR4 and their surface level were similar in WT and ρ^0 cells. However, enhancement of TLR4 expression on plasma membrane in response to LPS was significantly suppressed in ρ^0 cells as compared with that in RAW cells (Supplementary Fig. 3). At this point, we can not exclude the possibility that an absence of mitochondria affects the formation of TLR4-LPS complex activating signal cascade to induce cytokines and NO production. This possibility should be studied further.

In addition to mitochondrial ROS generation, another important source inducing ROS generation in response to LPS is NADPH oxidase [24,25]. The NADPH oxidase complex is known to be a major producer of extracellular and/or intracellular ROS generation in neutrophil and phagocyte. It has been reported that NADPH oxidase-dependent ROS generation mediates amplified LPS response via enhancement of TLR4 trafficking to the cell membrane [25]. In the present study, although secretion of TNF-α in response to LPS was not affected in the presence of NADPH oxidase inhibitor (Fig. 2A), LPS-induced IL-6 production was slightly suppressed by inhibition of NADPH activity (data not shown). This result suggests the possibility that NADPH oxidase-induced ROS generation is partially involved in the secretion of IL-6, although the effect was less than those by inhibition of intracellular ROS generation.

As mitochondria constantly generate superoxide radical and related ROS under physiological condition, it might become the predisposing condition for quick response to combat microbial infection. Our results demonstrated that mitochondrial density might be critical in responsiveness to LPS-induced macrophage activation, in part, via regulation of ROS production, which may reveal novel mitochondrial function in immune systems against invasion.

Acknowledgements

We thank the members of our laboratory for technical support and helpful discussion. We also thank to Dr. Takayuki Kato, Department of Physiology, Osaka City University Graduate School of Medicine for his kind cooperation and helpful discussion. This work was supported by grants from the Ministry of Education, Science, Sports and Culture of Japanese Government (21700698 for E.K.).

Appendix A. Supplementary data

Supplementary data associated with this article can be found, in the online version, at doi:10.1016/j.febslet.2011.05.049.

References

[1] Uematsu, S. and Akira, S. (2006) Toll-like receptors and innate immunity. J. Mol. Med. 84, 712–725.
[2] Roger, T. et al. (2009) Protection from lethal gram-negative bacterial sepsis by targeting Toll-like receptor 4. Proc. Natl. Acad. Sci. USA 106, 2348–2352.
[3] Kawai, T. and Akira, S. (2007) TLR signaling. Semin. Immunol. 19, 24–32.
[4] Kawai, T. and Akira, S. (2010) The role of pattern-recognition receptors in innate immunity: update on Toll-like receptors. Nat. Immunol. 11, 373–384.
[5] Weinstein, S.L., Sanghera, J.S., Lemke, K., DeFranco, A.L. and Pelech, S.L. (1992) Bacterial lipopolysaccharide induces tyrosine phosphorylation and activation of mitogen-activated protein kinases in macrophages. J. Biol. Chem. 267, 14955–14962.
[6] Han, J., Lee, J.D., Bibbs, L. and Ulevitch, R.J. (1994) A MAP kinase targeted by endotoxin and hyperosmolarity in mammalian cells. Science 265, 808–811.
[7] Guha, M. and Mackman, N. (2001) LPS induction of gene expression in human monocytes. Cell Signal. 13, 85–94.
[8] Cakir, Y. and Ballinger, S.W. (2005) Reactive species-mediated regulation of cell signaling and the cell cycle: the role of MAPK. Antioxid. Redox Signal. 7, 726–740.
[9] Kamata, H. and Hirata, H. (1999) Redox regulation of cellular signalling. Cell Signal. 11, 1–14.
[10] Chance, B., Sies, H. and Boveris, A. (1979) Hydroperoxide metabolism in mammalian organs. Physiol. Rev. 59, 527–605.
[11] Emre, Y., Hurtaud, C., Nubel, T., Criscuolo, F., Ricquier, D. and Cassard-Doulcier, A.M. (2007) Mitochondria contribute to LPS-induced MAPK activation via uncoupling protein UCP2 in macrophages. Biochem. J. 402, 271–278.
[12] Emre, Y. and Nubel, T. (2010) Uncoupling protein UCP2: when mitochondrial activity meets immunity. FEBS Lett. 584, 1437–1442.
[13] Qian, W., Nishikawa, M., Haque, A.M., Hirose, M., Mashimo, M., Sato, E. and Inoue, M. (2005) Mitochondrial density determines the cellular sensitivity to cisplatin-induced cell death. Am. J. Physiol. Cell Physiol. 289, C1466–C1475.
[14] King, M.P. and Attardi, G. (1989) Human cells lacking mtDNA: repopulation with exogenous mitochondria by complementation. Science 246, 500–503.
[15] Wang, D., Malo, D. and Hekimi, S. (2010) Elevated mitochondrial reactive oxygen species generation affects the immune response via hypoxia-inducible factor-1alpha in long-lived Mclk1+/- mouse mutants. J. Immunol. 184, 582–590.
[16] Arsenijevic, D. et al. (2000) Disruption of the uncoupling protein-2 gene in mice reveals a role in immunity and reactive oxygen species production. Nat. Genet. 26, 435–439.
[17] Alves-Guerra, M.C. et al. (2003) Bone marrow transplantation reveals the in vivo expression of the mitochondrial uncoupling protein 2 in immune and nonimmune cells during inflammation. J. Biol. Chem. 278, 42307–42312.
[18] Bai, Y. et al. (2005) Persistent nuclear factor-kappa B activation in Ucp2-/- mice leads to enhanced nitric oxide and inflammatory cytokine production. J. Biol. Chem. 280, 19062–19069.
[19] Azzu, V. and Brand, M.D. (2010) Degradation of an intramitochondrial protein by the cytosolic proteasome. J. Cell Sci. 123, 578–585.
[20] Selimovic, D., Hassan, M., Haikel, Y. and Hengge, U.R. (2008) Taxol-induced mitochondrial stress in melanoma cells is mediated by activation of c-Jun N-terminal kinase (JNK) and p38 pathways via uncoupling protein 2. Cell Signal. 20, 311–322.
[21] McGettrick, A.F. and O'Neill, L.A. (2010) Localisation and trafficking of Toll-like receptors: an important mode of regulation. Curr. Opin. Immunol. 22, 20–27.
[22] Nakahira, K. et al. (2006) Carbon monoxide differentially inhibits TLR signaling pathways by regulating ROS-induced trafficking of TLRs to lipid rafts. J. Exp. Med. 203, 2377–2389.
[23] Powers, K.A., Szaszi, K., Khadaroo, R.G., Tawadros, P.S., Marshall, J.C., Kapus, A. and Rotstein, O.D. (2006) Oxidative stress generated by hemorrhagic shock recruits Toll-like receptor 4 to the plasma membrane in macrophages. J. Exp. Med. 203, 1951–1961.
[24] Park, H.S., Jung, H.Y., Park, E.Y., Kim, J., Lee, W.J. and Bae, Y.S. (2004) Cutting edge: direct interaction of TLR4 with NAD(P)H oxidase 4 isozyme is essential for lipopolysaccharide-induced production of reactive oxygen species and activation of NF-kappa B. J. Immunol. 173, 3589–3593.
[25] Kong, X., Thimmulappa, R., Kombairaju, P. and Biswal, S. (2010) NADPH oxidase-dependent reactive oxygen species mediate amplified TLR4 signaling and sepsis-induced mortality in Nrf2-deficient mice. J. Immunol. 185, 569–577.

日本細菌学雑誌
66（4）：531–537，2011

平成23年小林六造記念賞受賞論文

結核菌の病原性および増殖制御機構の分子遺伝学的解析と応用研究

松　本　壮　吉[1]

[1] 大阪市立大学大学院医学研究科細菌学分野
〒545–8585　大阪府大阪市阿倍野区旭町 1–4–3

結核菌は，飛沫核感染によって，肺を侵入門戸としてヒトに感染する。感染者の約 5%が速やかに結核を発症するが，多くの場合（感染者の約 95%），無症候感染が成立する。ヒト型結核菌は，ヒトに特化した寄生病原体であり，感染成立後，免疫系は菌を生体から駆逐することができない。現在，無症候感染者は人類の 1/3 にのぼると推定されている。結核菌をはじめ，ヒトに寄生する病原性抗酸菌は遅発育性である。さらに潜伏感染菌の多くは，増殖を停止しているが死滅しない休眠状態に移行する。遅発育性や休眠現象は，疾患の慢性化や宿主—菌双方の長期生存につながる病原性抗酸菌に特徴的な形質である。一方，無症候結核菌感染者の 5–10%で感染菌の再増殖，すなわち内因性再燃が生じる。成人肺結核の多くがこの機序で発症し，現在，年間約 100 万人以上の命が失われている。このように結核の無症候化（潜在化）と発症は，結核菌自身の増殖と密接にリンクする。以上の背景のもと，結核菌の病原性解析のベースとなる，抗酸菌の宿主ベクター系の構築とその応用を図るとともに，菌の増殖制御メカニズムを解析し，結核菌の生体内増殖を促進する宿主分子や，菌自身の遅発育性や休眠現象に関わる増殖抑止蛋白質を同定した。

結核（症）の歴史と現状

結核の痕跡として古いものに，ドイツで発見された紀元前 7,000 年頃のミイラに残る脊椎カリエスであるが，結核菌の誕生は更にさかのぼり，ゲノム解析によると，アフリカにおける人類の誕生と同時期に近縁菌より進化し，人の移動に伴って古代には陸路で，人類が船を使うようになってからは海路で世界に伝播したと推定されている（14, 34）。戦後の急速な結核罹患率の低下から惰性的に制圧されると楽観された時期もあったが，AIDS の蔓延によって発展途上国における結核の脅威は増大し，さらに先進国においても多剤耐性結核菌の出現などが災いして日本を含め罹患率が再上昇する国もあらわれた。最新の統計によると，2010 年には，880 万人が新たに結核に罹患し，140 万人が死亡している。国内でも 23,261 人が新たに患者として登録され，2,126 人が死亡しているように，結核は現在も，世界／国内ともに最大級の細菌性感染症である。

Sohkichi MATSUMOTO
Analysis of molecular mechanisms of the virulence and growth coordination of *Mycobacterium tuberculosis*
Department of Bacteriology, Osaka City University Graduate School of Medicine, 1–4–3 Asahi-machi, Abeno-ku, Osaka 545–8585

潜在性結核—休眠現象—内因性再燃

結核菌は抗酸菌属に分類されるグラム陽性の桿菌である。抗酸菌の中で特に生体内での生存力に優り，実験的にはマウスやモルモットに経気道的感染で簡単に動物を死に至らしめる。自然宿主のヒトに対しては，初感染で発病するケースは 5%以下と稀であるが，感染した菌は免疫応答に屈することなく生体内で生存し続ける（図 1）（6）。このように長期間潜伏感染する菌をパーシスターと呼ぶ。パーシスターの多くは休眠（dormancy）菌で，通常は発症に至らないが，宿主の抵抗性の低下などにより，再び増殖を開始し結核を発症する（図 1）。成人の肺結核の多くは内因性再燃により，感染者の 5–10%が結核を発症する。現在，20 億人に人類に結核菌が感染しており，今後 20 年間で 2 億人が発病すると予測されている。このような発症のリスクを背負っていることから，無症候の結核菌感染は潜在性結核と定義される。

抗酸菌の宿主—ベクター系の開発と応用

私は大学を卒業後，当時，山田　毅先生が主宰されていた長崎大学の口腔細菌学教室所属の大学院生として研究を始めた。山田研究室では，抗酸菌の病原性に関わる分泌蛋

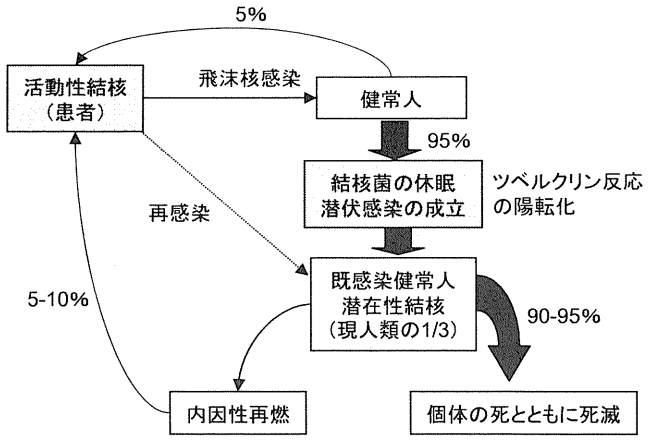

図1. 結核菌の生活環と結核の発病
結核患者由来の菌を含有する飛沫核が健常人の肺胞に到達し感染が成立する。感染者の5%程度が結核を発症し，残りの95%は無症候キャリアとなるが，菌は生体から排除されない。潜在期において結核菌は，増殖を停止した休眠菌となり，菌—宿主双方の生存が保証される。現在人類の1/3が潜在性結核とされており，HIV非感染者で終生の間5–10%が，HIV- 結核菌感染者で年間10%が結核を発症する。

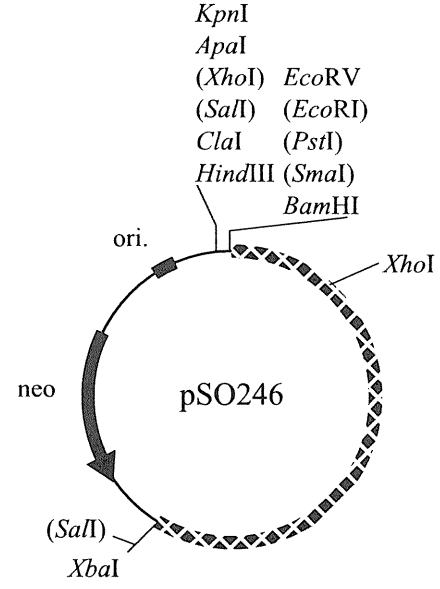

図2. 抗酸菌—大腸菌シャトルプラスミドpSO246
pAL5000由来抗酸菌プラスミド（網掛け），*neo*（カナマイシン耐性遺伝子），ori（大腸菌内複製起点）をつなげたもの。利用できる制限酵素サイトを図中に示す。全長4407 bp。（文献20より一部改変）。

白質の解析が行われていた。抗酸菌分子生物学の黎明期であった当時，国内での抗酸菌遺伝子の解析は困難で，大腸菌で用いられているベクター系を利用できない状況にあったが，私は，宿主—ベクター系の確立に関わる幸運に恵まれた。

Mycobacterium fortuitum 由来のpAL5000プラスミドの複製起点(28)，放線菌由来のカナマイシン耐性遺伝子，大腸菌プラスミドの複製起点をつなぎ，抗酸菌—大腸菌のシャトルプラスミドを作成した。当初作製したシャトルプラスミドは，複製時において頻繁な脱落が観察されたが，機能に不要な部位を削除していくことで安定化をはかり，野生プラスミドであるpAL5000並にダウンサイジングしたpSO246（4.4 kbp）を構築した(20)（図2）。pSO246は抗酸菌内で安定に複製することが証明され，薬剤の選択圧のない環境下でも，一定に保持された。さらに，山田研究室でクローニングされていた抗酸菌の主要分泌蛋白質（alpha antigenもしくはAntigen 85B)(24, 26)を利用して遺伝子を安定的に発現できることを示し，抗酸菌の宿主—ベクター系を構築した(20)。

次に，組み換え抗酸菌技術を，新しい予防法や治療法開発への利用を図る研究に従事した。結核ワクチンであるBCGは，強いアジュバント活性を有し，長期間の免疫付与が可能で，安価で安全であるという特性を有する。したがい，抗酸菌の組換え技術を利用してBCGを改変／改良し，難病の予防や治療への応用することが期待されていた(1, 25, 30)。

マラリア原虫メロゾイト期の主要な表面抗原にmerozoite surface protein 1（MSP1）という赤内型マラリア（赤血球感染期）に対する防御抗原として注目される蛋白質がある。MSP1は，複数回のプロセシングの後に，システイン結合で高次の立体構造をとり，カルボキシル末端のみがメロゾイト表面に繋留される。防御抗体の産生には，本来の立体構造を有するMSP1抗原の必要性が指摘されていた(4, 5)。我々はBCGからMSP1のカルボキシル末端部の発現を試みた。抗酸菌分泌蛋白質alpha抗原（Antigen 85B）との融合蛋白質として分泌されたMSP1は，適切な立体構造をとることが，原虫感染時の抗血清反応により判明した(22)。これは，MSP1を菌体外に分泌させたことが功を奏したものと考えられた。

感染実験において，MSP1を発現する組み換えBCGをマウスに投与することでマウスの一定の種において，原虫感染後の生存率が飛躍的に上昇することが判明した（図3）。次に，防御免疫を付与できるマウスとそうでないマウスの

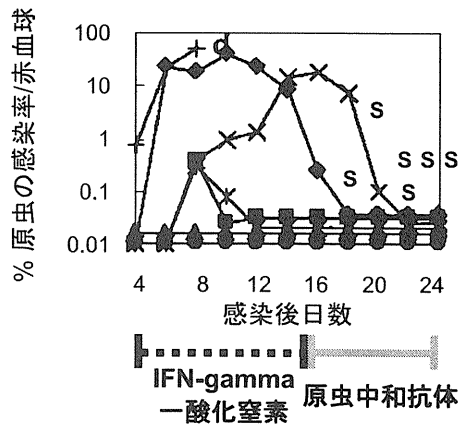

図3. 組み換えBCGによるマラリアに対する防御応答の誘導
MSP1を発現する組み換えBCGをC3H/HeJマウスに免疫し，マウスマラリア原虫である*Plasmodium yoelii* 17XL（致死株）を感染させた。感染初期には，MSP1に対するIFN-gammaとNO産生が，後期には，原虫中和抗体が産生され，マウスはマラリアによる死を免れる。（文献22より一部改変）。

差異を解析し，原虫感染初期にインターフェロンγの産生が生じ，その後，速やかに中和抗体（原虫の赤血球侵入を阻害する）が産生されると，病気が治癒することを突き止めた(22, 23)。本成果は，BCGがマラリアワクチンのベクターとして有用であることに加え，原虫抗原に対する抗体応答以外に，細胞性免疫応答の惹起も感染防御に必須であることを示し，マラリアのワクチン開発においても重要な情報を提供することとなった。

同様にBCGの組み換え技術を利用し，膀胱癌の治療やHIV感染症の予防ワクチンの開発を促した。サイトカインを産生する組換えBCGにより細胞傷害性T細胞の活性化をより促進し，膀胱癌細胞株に対する傷害活性を増強させたり(35)，HIVの構造蛋白質や外套蛋白質のエピトープをBCGから発現させ，構築した抗酸菌の宿主ベクター系を用いることで，長期間の防御免疫を付与できることが実証された(2)。

結核菌のII型肺胞上皮細胞への感染とヒアルロン酸を利用した増殖

結核菌の侵入門戸は肺で，菌を含んだ飛沫核が肺胞に到達することで感染が成立する。肺胞内腔表面は3種の細胞により形成されるが，結核菌の標的は肺胞マクロファージとII型肺胞上皮細胞である。前者に対して菌は，コレステロール依存的に補体レセプターやマンノースレセプターを介して侵入する(11)。一方，II型肺胞上皮細胞への感染においては，グリコサミノグリカンの重要性が示されていた(27)。

私たちは，結核菌がII型肺胞上皮細胞にグリコサミノグリカンの中でもヒアルロン酸を利用して感染することを明らかにした(3)。さらに感染成立後にも，ヒアルロン酸の存在によって菌の増殖が促進されることを見出した(15)。

ヒアルロン酸は，N-アセチルグルコサミンとグルクロン酸からなる高分子の直鎖多糖である。細胞外マトリックスの主成分として知られるが，気道にも存在し粘膜せん毛エレベーターに拮抗して抗菌物質を繋留するなど，気道系の防御に重要な役割を果たしている(12)。

ヒアルロン酸による結核菌の増殖増強の機構を解析した結果，結核菌はヒアルロン酸を分解し炭素源として利用することを明らかにした。ヒトは3種類のヒアルロン酸合成酵素（HAS）を産生するが，その中でも結核菌は合成能の旺盛なHAS2ではなく，HAS1によって合成される短鎖ヒアルロン酸を効率良く増殖に利用した。結核菌感染肺においては，驚いたことにHAS2ではなくHAS1の顕著な発現が認められ，サルやヒトの結核病変（肉芽種）にはヒアルロン酸の蓄積が観察された（図4）。

結核におけるヒアルロン酸の重要性はこれまで指摘されたことはなかった。ヒアルロン酸は，D-*N*-アセチルグルコサミンとD-グルクロン酸が交互に結合した直鎖状の高分子多糖である。肺実質の細胞外マトリックスの主要成分で肺組織の形成に関わると同時に，粘膜下腺の漿液細胞から気道内に分泌される。肺から気道にかけては，粘膜繊毛装置により粘液は終止口蓋にむけて移動し感染や汚染を防いでいる。分泌されたヒアルロン酸は，気道表面に存在するヒアルロン酸レセプター（RHAMM）に結合して留まり，リゾチームなどの抗菌物質を粘膜繊毛装置に逆らって特異的に繋留させることで気道の無菌化に重要な役割を果たす(12)。一方，肺胞内粘液中にもヒアルロン酸は存在し，CD44レセプターを介して肺胞マクロファージに補食される(10)。つまり，結核菌が感染する気道系内腔表面はヒアルロン酸が豊富に存在し，菌がヒアルロン酸を利用するということは，極めて理にかなっている。これまで結核におけるヒアルロン酸の役割は見過ごされてきたが，本データはヒアルロン酸が結核病態の形成に重要な役割を担うことを示唆しており，結核研究や治療法開発における新たな視点を提示している(3, 15)。

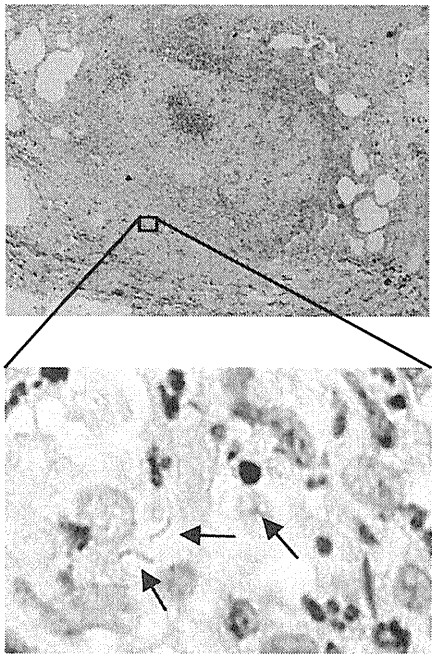

図4. 結核で死亡したサル肺肉芽腫腫における結核菌とヒアルロン酸
結核で死亡したアカゲ猿肺の肉芽腫切片をアルシアンブルー染色（青色，グリコサミノグリカンを染色）と抗酸性染色を行ったもの。同切片のアルシアンブルー染色は，ヒアルロン酸分解酵素で，染色性の多くが失われることから，サル結核肉芽腫にヒアルロン酸が蓄積し，ヒアルロン酸の存在部位に結核菌が存在することが分かる。（文献15より一部改変）。

結核菌の増殖制御のメカニズム解析

一般に細菌は，適切な栄養条件下で迅速に分裂して繁殖する進化をとげたと考えられるが，抗酸菌は例外的に緩慢に増殖する細菌である。自然環境下での生存に不利であるが，抗酸菌のような寄生生物にとっては宿主との共存に有利に働く。抗酸菌は，休眠（dormant）期へと移行し，増殖を停止した後にも長期間生存することができる。成人肺結核の多くは休眠菌の再増殖であることから，菌の増殖制御は疾患の沈静化や発症とも密接に繋がる。このような遅

発育性や休眠現象は，抗酸菌に特徴的なの生命現象であり，未知の研究領域であった。

大学院で分子生物学を学んだ背景から，生物の設計図は遺伝子に記されており，その遺伝子発現の制御で細胞の機能や運命が変わるのであれば，遺伝子の発現制御から生命現象を観察したいという想いがあった。それで，抗酸菌の遅発育性や休眠現象の解明を，遺伝子発現の調節を行うと想定されるDNA結合性分子の探索を足がかりとして始めた。

細胞内で菌は低酸素状態に曝され，その結果，結核菌の増殖停止と休眠が促進されると考えられている(33)。Barry等は低酸素状態での蛋白質発現プロファイルを解析し，αクリスタリン様の蛋白質（Acr）が顕著に発現誘導されることを見いだした(37)。このAcrが現在，結核菌の休眠マーカーとして利用されている。Acrは，眼球レンズの曇りをとる蛋白質と相同性を有する分子，すなわち分子シャペロンであり，休眠菌内部で蛋白質の変性を防いでいると推測される。

Acrを発現している牛型結核菌の弱毒株であるBCGの菌体蛋白質を解析し，最も大量に発現している蛋白質を同定した。抗酸菌特異的に普遍的に存在する分子で，DNA結合性蛋白質であることからmycobacterial DNA-binding protein 1（MDP1）と名付けた（特許第4415200号）(21)。MDP1は，N末端領域は大腸菌の核酸結合性蛋白質HUと，C末端領域はヒトを含む哺乳類のヒストンH1蛋白質と部分的相同性を有し，菌体内では核酸と50Sリボゾームに結合していた。

増殖には，酵素の発現とDNA合成が必須であるので，RNA合成，蛋白質合成，さらにDNA合成に対するMDP1の作用を，試験管内の高分子合成系を用いて検討した。その結果，MDP1は転写，翻訳，複製いずれも強く抑制することが判明した(18)（図5）。

MDP1の転写および複製阻害は，核酸の競合阻害により減弱することから，核酸結合性に依存している。合成ペプチドを用いた解析から31–50のアミノ酸領域に強い核酸結合性があることが分かり，アミノ酸置換により結合モチーフをTIxxAVxxGxxVTIxxFxxx（xは置換可能なアミノ酸）と決定した(13)。この配列は，MDP1に特異的であり，抗酸性を示す近縁の*Nocardia*や*Rhodococcus*以外に他の生物の持つ核酸結合性蛋白質には存在しない。抗酸菌はグアニンとシトシンに富むGC-richなゲノムを有するが，このモチーフ配列はグアニンとシトシンを介して核酸と結合する。そしてMDP1と同様にRNA合成とDNA合成を阻害する。これらの結果から，31–50領域がMDP1の主要なDNA結合領域であり，転写／複製阻害を担う活性部位であると推測された(13)。

次にMDP1を大腸菌や，速育型の抗酸菌である*M. smegmatis*，さらに遅発育性のBCGに発現させると，それぞれ菌の増殖を抑制することが分かった(16, 18)（図5）。余談であるが，MDP1を発現させて増殖が緩慢となった寒天培地上の菌を山田　毅先生の奥さん（和子様）にお見せし，

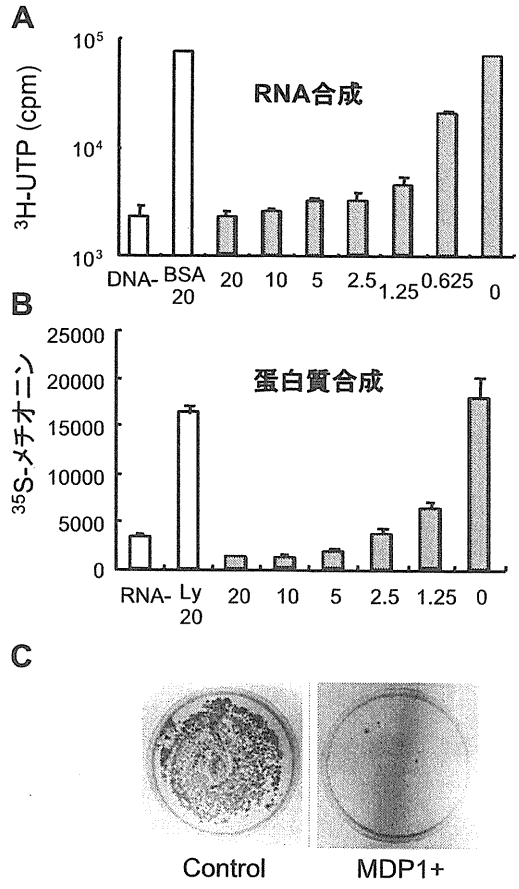

図5. MDP1は転写／翻訳を阻害し，菌の増殖を抑制する
A, MDP1によるRNA合成阻害。縦軸は，RNAの合成量を^{3}H-dUTPの取り込み量で表している。MDP1を20, 10, 5, 2.5, 1.25および0 μMそれぞれ加えた。RNA合成酵素はT7ファージ由来のものを用いた。B, MDP1による蛋白質合成阻害。縦軸は，蛋白質合成量を^{35}S-メチオニンの取り込み量で表している。大腸菌リボゾームとファージRNAを鋳型に蛋白質合成を行った。C, BCG由来のMDP1を発現した*M. smegmatis*（MDP1+）を寒天培地にて増殖させたもの。コントロール（左）に比べ，増殖が顕著に抑制される。（文献18より一部改変）。

驚いていただいたことが今も忘れられない。MDP1は結核菌では生存自体に必須と推測されており(29)，通常の方法では欠失株の作成は不可能であるが，ドイツのLewin等が，MDP1の発現をアンチセンスにより50%程度減衰させることに成功した。このMDP1の発現量の低下により，牛型結核菌弱毒株BCGの増殖が加速することが示され，低酸素環境において様々な遺伝子発現や糖脂質合成のパターンが変化することが示された(17)。これらの成績から，MDP1は抗酸菌の遅発育性や休眠現象を説明する有力な分子の一つであることが判明した。

MDP1の鉄貯蔵とフェロキシダーゼ活性

鉄は，呼吸や核酸合成酵素の活性中心として生物に利用されており，多くの生物に必須の金属である。これは，生理的な環境下で容易に電子を授受（$Fe^{2+} \rightleftarrows Fe^{3+}$）できる性質によるが，鉄の細胞毒性もこの性質によって容易に生じる。すなわち，Fe^{2+}は，過酸化水素の存在下で最も活性の高い酸素ラジカル“ヒドロキシラジカル”をフェントン反

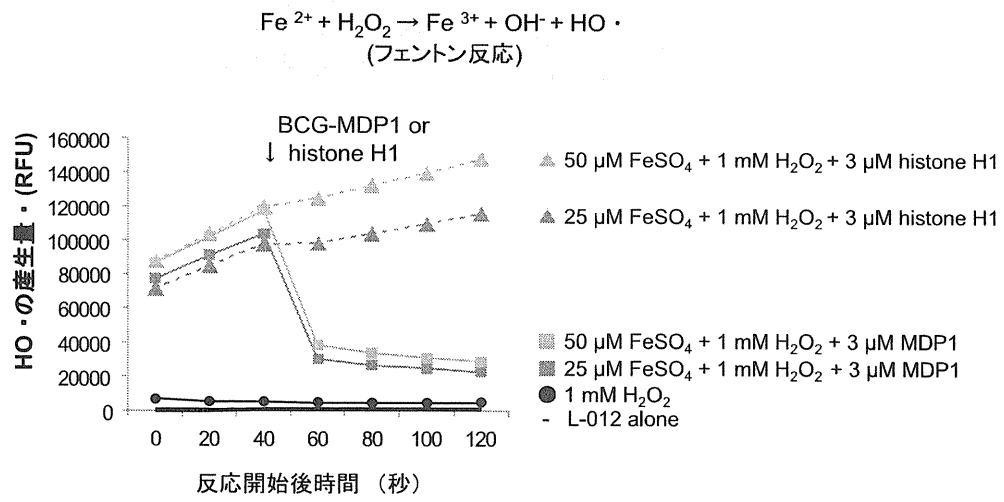

図 6. MDP1 は，フェントン反応によるヒドロキシラジカル（HO・）の産生を抑制する
2 価鉄と酸素呼吸の副次反応の結果生じる H_2O_2 が反応（フェントン反応）し，最も毒性の高い酸素ラジカルであるヒドロキシラジカルが生じる。フェントン反応系に，MDP1 を加える（40 秒後）とヒドロキシラジカルの産生が顕著に抑制される。対照蛋白質（ヒストン H1）にそのような活性はない。ヒドロキシラジカルの産生は，L-012 をプローブとして測定した。（文献 31 より一部改変）。

応により発生させる。一方，Fe^{3+} は安定であるが溶解性に乏しく（10^{-18}M），生体が必要とする鉄濃度（10^{-7}M）にほど遠い (8)。したがい生物は，鉄代謝を厳密に調節する必要があり，Ferritin-super family 蛋白質は，その中心的な役割を果たしている。Ferritin-super family 蛋白質は 12 もしくは 24 量体で，鉄酸化活性によってフェントン反応を回避し，内部にミネラル（Fe^{3+}）として 800–4,500 原子の鉄を貯蔵する (7)。Ferritin はマウスや人でも生存に必須の分子であり，欠失した生体は生存しない。

結核菌は，DNA 結合性のフェリチン様蛋白質を有さないが (9)，我々は MDP1 にフェリチン様活性，すなわち鉄酸化活性と貯蔵性があることを見いだした (31)。結核菌 MDP1 のフェロキシダーゼ活性 K_m 値は 0.252 mM で，1 蛋白質あたり 138.7±35.5 の鉄原子を貯蔵する。Ferritin-super family 以外の分子に，フェリチン様活性を見いだした初めての報告となった (31)。MDP1 はヒストン様蛋白質でフェリチンとは分子のルーツが異なることから，抗酸菌は進化の過程で独自にフェリチン様活性を有するヒストン様蛋白質を獲得したと推測される。MDP1 は，フェロキシダーゼ活性によりフェントン反応を回避して（図 6），DNA などを障害するラジカルの産生を抑制した (31)。酸素ラジカルの消去能は，生物の寿命と相関するといわれる (32)。休眠期結核菌内で MDP1 は，菌の増殖を停止させると同時に，酸素ラジカルの発生回避を介して，潜伏結核菌の長期生存に寄与することが想定される。

終わりに，今後の研究展開

人類の 1/3 に増殖を停止した休眠結核菌が感染していると推定されている。そして，成人の肺結核の多くは内因性再燃により，感染者の 5–10%が終生の間に結核を発症することから，今後 20 年間で 2 億人が発病すると予測されている。

一方，ヒト型結核菌はヒトに特化した寄生体であり，ヒト以外の生体や環境中には，例外を除き生存しない。また結核菌が世代を継ぐには，発症し飛沫核感染で，新たな宿主に感染することが必要である。潜在化のままでは，宿主の死とともに感染菌も死滅してしまうからだ。したがい活動性結核に対処するとともに，病原体の源泉である潜在性結核からの内因性再燃を抑止することが，結核の制圧につながる。

私たちは，抗酸菌 DNA で最初に見つけられた DNA のアジュバント活性と相まって (36)，MDP1 と DNA 複合体に強い抗原性があることを動物レベルで明らかにしているが (19)，ヒトでは，潜在性結核においても MDP1 に対する顕著な免疫応答が生じていること，および MDP1 が実際に非発症者の肺で発現していることが厚生労働省科学研究にて（研究代表　小林和夫先生）明らかになりつつある。MDP1 などの潜在期抗原は，成人性肺結核に有効な内因性再燃を抑止するワクチンとなる可能性もある。今後，結核菌の増殖制御のメカニズムという基礎科学から，結核の潜在化と発症の機構を解明し，さらには，MDP1 のような増殖抑止分子等の潜在化のメカニズムを利用した，結核の制圧原理の確立と実践を進めていきたい。

また単細胞でありながら長期の生存が可能な結核菌の休眠現象に，生物に普遍の“生き続ける”ための機構があるのであれば，その秘密を解き，ヒトの長寿に応用したいと考える。

謝　　辞

本研究を遂行するにあたり，これまでに，親身になってご指導いただきました，長崎大学歯学部口腔細菌学講座教授　山田　毅先生（現名誉教授）と，大阪市立大学大学院医学研究科感染防御学（現細菌学）分野　前教授の小林和夫先生（現国立感染症研究所免疫部長）に深く感謝いた